

Accepted Manuscript

Discovery of new indomethacin-based analogs with potentially selective cyclooxygenase-2 inhibition and observed diminishing to PGE2 activities

Shaymaa E. Kassab, Mohammed A. Khedr, Hamed I. Ali, Mohamed M. Abdalla



PII: S0223-5234(17)30771-7

DOI: [10.1016/j.ejmech.2017.09.056](https://doi.org/10.1016/j.ejmech.2017.09.056)

Reference: EJMECH 9771

To appear in: *European Journal of Medicinal Chemistry*

Received Date: 25 June 2017

Revised Date: 21 September 2017

Accepted Date: 26 September 2017

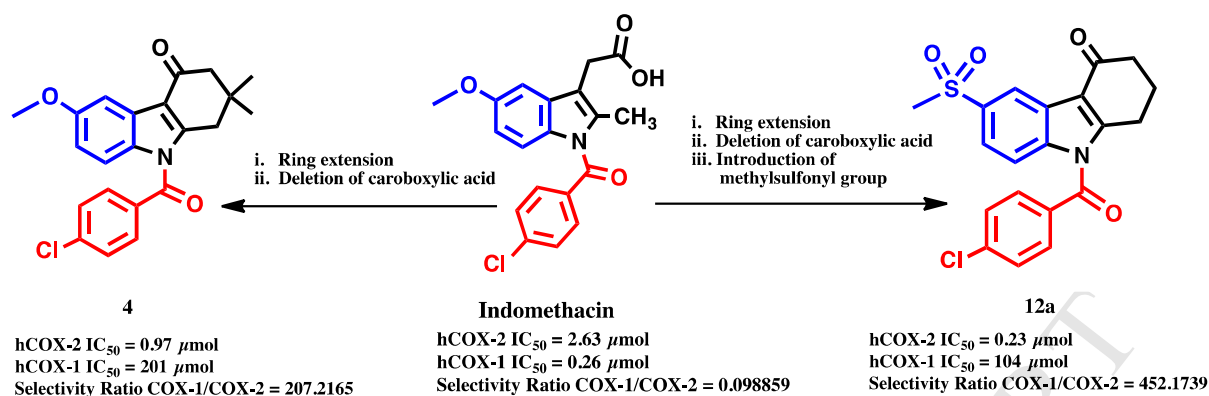
Please cite this article as: S.E. Kassab, M.A. Khedr, H.I. Ali, M.M. Abdalla, Discovery of new indomethacin-based analogs with potentially selective cyclooxygenase-2 inhibition and observed diminishing to PGE2 activities, *European Journal of Medicinal Chemistry* (2017), doi: 10.1016/j.ejmech.2017.09.056.

This is a PDF file of an unedited manuscript that has been accepted for publication. As a service to our customers we are providing this early version of the manuscript. The manuscript will undergo copyediting, typesetting, and review of the resulting proof before it is published in its final form. Please note that during the production process errors may be discovered which could affect the content, and all legal disclaimers that apply to the journal pertain.

Discovery of New Indomethacin-based analogs with Potentially Selective Cyclooxygenase-2 Inhibition and Observed Diminishing to PGE2 activities.Shaymaa E. Kassab^{a*}, Mohammed A. Khedr^b, Hamed I. Ali^{b,c}, Mohamed M. Abdalla^d^aPharmaceutical Chemistry Department, Faculty of Pharmacy, Damanhour University, Damanhour, El-Buhaira 22516, Egypt.^bPharmaceutical Chemistry Department, Faculty of Pharmacy, Helwan University, Ein Helwan, Cairo 11795, Egypt.^cDepartment of Pharmaceutical Sciences, Texas A&M University Irma Lerma Rangel College of Pharmacy Kingsville 78363, Texas, USA.^dResearch Unit, Saco Pharm. Co., 6th of October City, Giza 68330, Egypt.**Abstract**

New ring-extended analogs of indomethacin were designed based on the structure of active binding site of both COX-1 and COX-2 isoenzymes and the interaction pattern required for selective inhibition of COX-2 to improve its selectivity against COX-2. The strategy adopted for designing the new inhibitors involved i) ring extension of indomethacin to reduce the possibility of analogs to be accommodated into the narrow hydrophobic tunnel of COX-1, ii) deletion of carboxylic acid to reduce the possibility of inhibitor to form salt bridge with Arg120 and eventually prevent COX-1 inhibition, and iii) introduction of methylsulfonyl group to increase the opportunity of the analogs to interact with the polar side pocket that's is crucial for inhibition process of COX-2. The three series of tetrahydrocarbazoles involving **4**, **5**, **9**, **10** and **12** were synthesized in quantitative yields adopting limited number of reaction steps, and applying laboratory friendly reaction conditions. *In vitro* and *in vivo* assays for data profiling the new candidates revealed the significant improvement in the potency and selectivity against COX-2 of 6-methoxytetrahydrocarbazole **4** ($IC_{50} = 0.97 \mu\text{mol}$) to verify the effect of ring extension in comparison to indomethacin ($IC_{50} = 2.63 \mu\text{mol}$), and 6-methylsulfonyltetrahydrocarbazole **10a** ($IC_{50} = 0.28 \mu\text{mol}$) to verify the effect of ring extension and introduction of methylsulfonyl group. 9-(4-chlorobenzoyl)-6-(methylsulfonyl)-1,2,3,9-tetrahydro-4H-carbazol-4-one **12a** showed the most potential and selective activity against COX-2 ($IC_{50} = 0.23 \mu\text{mol}$) to be with superior potency to Celecoxib ($IC_{50} = 0.30 \mu\text{mol}$). Consistently, **12a** was the most active with all the other anti-inflammatory test descriptors and its activity in diminishing the PGE2 with the other analogs confirmed the elaboration of new class of selective COX-2 inhibitors beyond the diarylsulfonamides as a previously common class of selective COX-2 inhibitors. Molecular docking study revealed the high binding score of compound **12a** (-30.78 kcal/mol), with less clash contribution (7.2) that is close to indomethacin. Also, **12a** showed low conformation entropy score (1.40). Molecular dynamic (MD) simulation identified the equilibrium of both potential and kinetic energies.

Keywords: Indomethacin, Tetrahydrocarbazoles, COX-2 inhibitors, Molecular docking, PGE2



1. Introduction

Prostaglandins (PGs) and glucocorticoids are mediators that potentially implicated to the inflammation process. Non-steroidal anti-inflammatory drugs (NSAIDs) are potent inhibitors of prostaglandins production. NSAID is pharmacologically targeting cyclooxygenase (COX), or PGH synthase, which catalyzes the first step of arachidonic-acid metabolism[1, 2]. Two isoforms of the membrane COX proteins are identified[3, 4]: COX-1, which is constitutively expressed in most tissues, to which the production of prostaglandins is attributed to; and COX-2, which is induced by cytokines, mitogens and endotoxins in inflammatory cells[5], is implicated to the elevated levels of prostaglandins during the inflammation. The enzymatic activity of COX involves bis-oxygenation of arachidonic acid to PGG₂, which then reduced to PGH₂ in a peroxidase reaction by the same protein[6]. NSAIDs act at the cyclooxygenase active site, and most inhibit both COX-1 and COX-2 with minimal specificity[7], leading to serious complications such as gastric ulcers and renal toxicity[8]. It is worthy to mention that both COX-1 and COX-2 isoenzymes are of ~60% sequence identity[7, 9]. Consistent with the high sequence identity, overall COX-1 and COX-2 are structurally conserved (RMSD < 1.0 Å for all C α atoms)[10] with high significance. The structure consists of three distinct domains: *N*-terminal epidermal growth factor (EGF) domain, a membrane-binding motif, and the *C*-terminal catalytic domain which involves the COX and peroxidase active sites[11]. The COX active site, termed as the lobby of hydrophobic pocket, is found at *C*-terminal. The active site structures between human COX-1 (hCOX-1) and hCOX-2 are quite different; in COX-1, it is long tunnel-like space, and in COX-2, it has an accessibly extra space due to presence of what is called side pocket[12]. This is attributed to the amino acid residue Ile 522 (Ile523 in Murine COX-1) in hCOX-1 which is analogous to Val 509 (Val523 in Murine COX-2) in hCOX-2[13, 14] but bulkier (**Figure 1**)[15] in the hydrophobic space of COX-1[16]. In COX-2, the less hindered Valine side chain and the conformational changes at Tyr355 leaves the hydrophobic segment of the polar side pocket widely open (**Figure 1**).

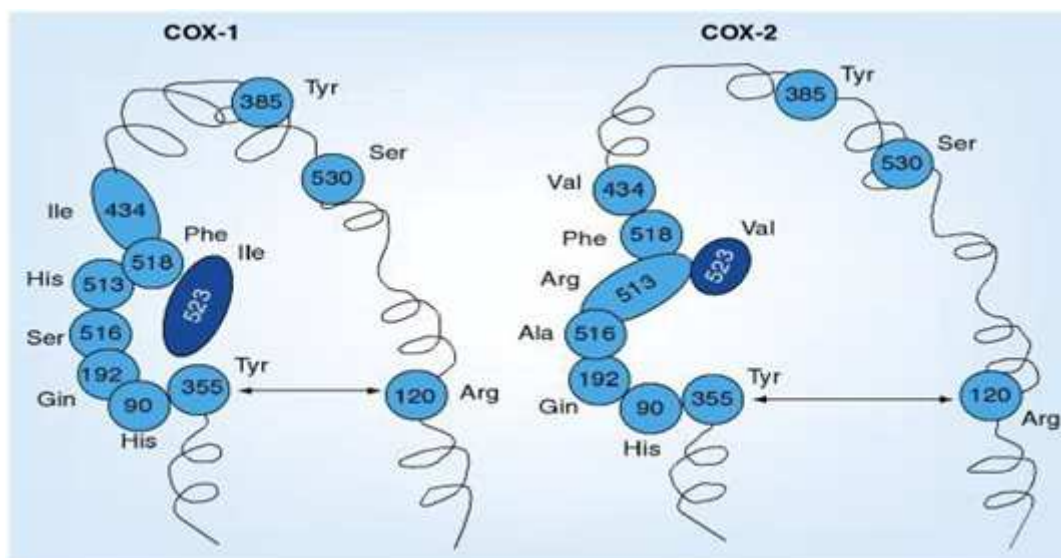


Fig. 1. Schematic comparison between COX-1 and COX-2 active binding sites.

The attempts for elaboration of selective COX-2 inhibitors are continued hoping to discover new inhibitors with less cardiovascular (CVS) side effects as a common problem of the whole class[12, 17, 18] that made Rofecoxib be withdrawn from the market. Thus, we selected indomethacin for the present study to be the lead compound upon which the design of the new analogs with improved selectivity against COX-2 is based.

Indomethacin, a classic non-selective COX inhibitor, binds deeply into the COX active site. Moreover, indomethacin penetrates furthest into the hydrophobic tunnel (**Figure 2a**)[19]. A 4-bromobenzyl analog, which lacks the benzoyl oxygen, shows high selectivity to COX-2 compared to indomethacin[20], suggesting that the benzoyl oxygen is important in enhancing the affinity to COX-1.

On the other hand, SC-558 (**Figure 2b**)[19], a diaryl heterocyclic inhibitor with a selectivity ratio > 375 for COX-1 over COX-2, has central pyrazole ring substituted by a sulfonamide substituent and attached to one of the aryl rings. In COX-2, there is a channel branches off at the Celecoxib binding site which leads from membrane to the COX active site[10]. One branch forms a cavity that contains the bromophenyl (tolyl in case of celecoxib) ring of SC-558, whereas the other represents a cavity not observed in COX-1 structure, and accommodates the entire phenylsulfonamide moiety (**Figure 2b**). Beyond the hydrophobic pocket, the sulfonamide group extends into the relatively polar side (selective) pocket near the surface of COX-2 (**Figure 2b**). The sulfonamide interacts with Gln178 (Gln192 in Murine COX-2), Leu338 (Leu352 in Murine COX-2) and Ser339 (Ser353 in Murine COX-2) amino acids of the polar side pocket via hydrogen bonding[16].

Reports recently recorded that the selectivity of COX-2 inhibitors is attributed to the phenyl sulfonamide moiety, which binds to the polar pocket that is not accessible in COX-1 but more accessible in COX-2, and remains vacant in complexes of COX-2 with non-selective inhibitors[15, 21-23]. In contrary, the carboxylate group that is a common group of various non-selective COX-inhibitors, is responsible for the conformational change of COX-1/2 via formation of salt bridge with the basic nitrogen of Arg120 (**Figure 2a**) and consequently non-selective inhibition of the enzyme is resulted[24].

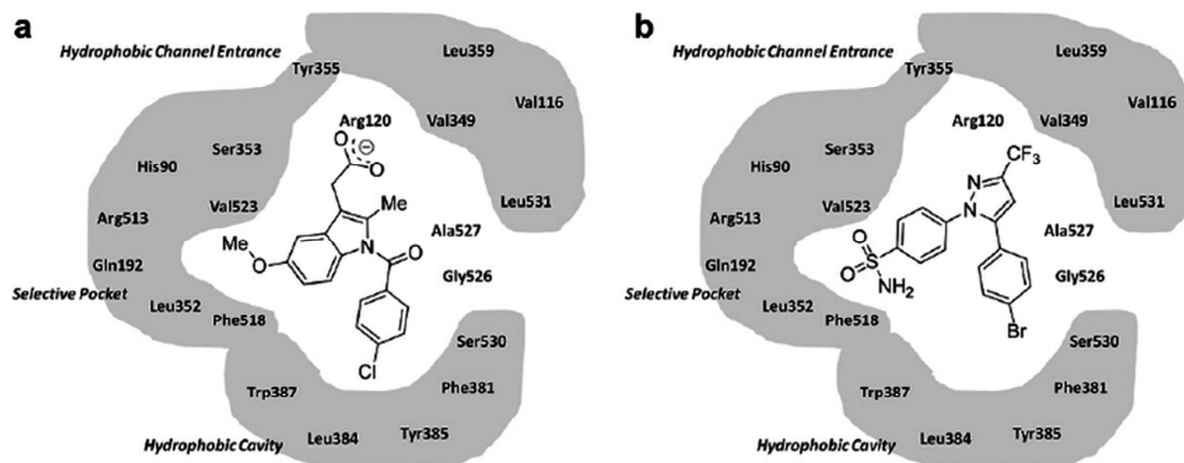


Fig.2. Schematic representation of SC-558 (COX-2 selective inhibitor) binding to COX-2 (a) and indomethacin (non-selective inhibitor) (b).

Interestingly, many potent diaryl-heterocyclic selective COX-2 inhibitors carried methylsulfonyl group[25, 26] instead of sulfonamide to confirm that the sulfone radical is the important fragment for interaction with the hydrophilic side pocket[23] and the oxidation state of the sulfur atom in sulfone form not sulfoxide as well. Consistently, it was reported that replacement of methoxy group with sulfamate group to one of indomethacin analogs at position 5 led to significant improvement in the selective COX-2 inhibition[27].

In view of the above findings, we have chosen the design of analogs to indomethacin prototype in which the acetic acid moiety is cyclized into cyclohexen-one/cyclohexene and in return the indole ring is extended into tetrahydrocarbazoles as a strategy and consequently deletion of carboxylic acid moiety, for improving the indomethacin selective COX-2 inhibition activity. The ring extension of indole ring of indomethacin attracted our attention aiming at proper binding of the new analogs into the wider hydrophobic[3][3]^[2a][28][3] lobby of COX-2 active binding site and reducing the opportunity of these analogs to bind into the narrower binding site counterpart in COX-1. Furthermore, salt bridge formation with Arg120 will never be accessible into COX-1 after the deletion of carboxylic acid. Thus, it has been suggested to generate 9-(4-chlorobenzoyl/benzyl/phenylsulfonyl)-6-methoxy-2,2-dimethyl-1,2,3,9-tetrahydro-4*H*-carbazol-4-ones [Figure 3 (Series I)]. Other derivatives of the analogs in which 6-methoxy group is replaced by 6-methylsulfonyl group affording 9-(4-chlorobenzoyl/benzyl/phenylsulfonyl)-6-methylsulfonyl-2,3,4,9-tetrahydro-1*H*-carbazoles [Figure 3 (Series II)] and 9-(4-chlorobenzoyl/benzyl/phenylsulfonyl)-6-(methylsulfonyl)-1,2,3,9-tetrahydro-4*H*-carbazol-4-ones [Figure 3 (Series III)]. This is to investigate the detrimental role of methylsulfonyl group in the conformational change of COX-2 in the inhibition process coupled with the ring extension in improving the selectivity of inhibition.

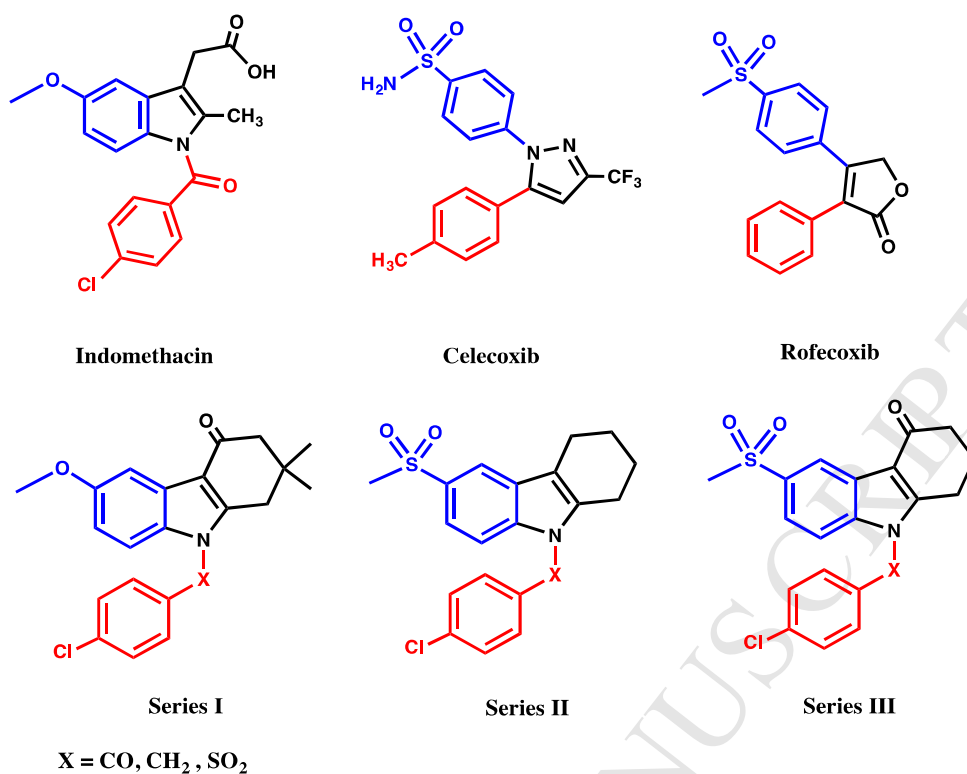


Fig. 3. Rational of the design of target selective COX-2 inhibitors (series I), (series II) and (series III)

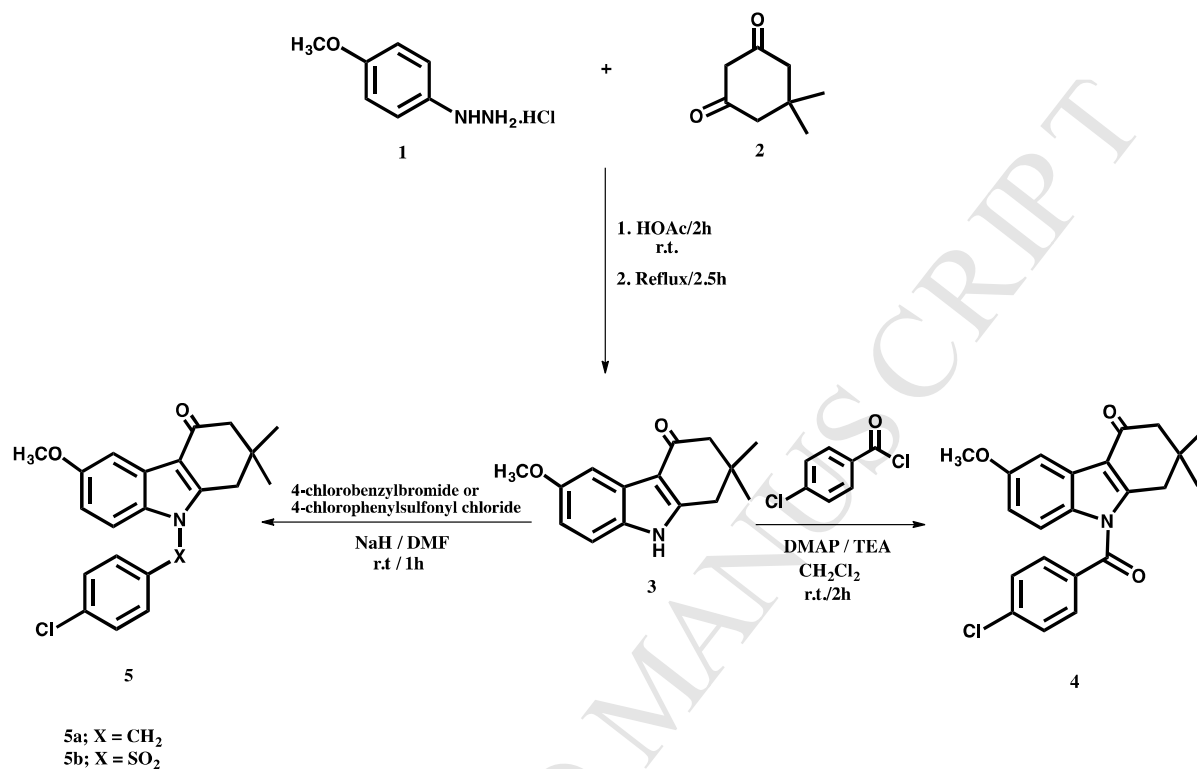
2. Results and discussion

2.1. Chemistry

The target COX-2 inhibitors 9-(4-chlorobenzoyl)-6-methoxy-2,2-dimethyl-1,2,3,9-tetrahydro-4*H*-carbazol-4-one **4**, 9-(4-chlorobenzyl)-6-methoxy-2,2-dimethyl-1,2,3,9-tetrahydro-4*H*-carbazol-4-one **5a** and 9-(4-chlorophenyl)sulfonyl)-6-methoxy-2,2-dimethyl-1,2,3,9-tetrahydro-4*H*-carbazol-4-one **5b** were synthesized according to **scheme 1**. The starting 6-methoxy-2,2-dimethyl-1,2,3,9-tetrahydro-4*H*-carbazol-4-one **3** was previously synthesized by Weng et al adopting a multi-step method to afford the tetrahydrocarbazole in a quantitative yield after long reaction time (12 hours) under reflux[28]. For us, we adopted another simple and one-step method starting with commercially available starting materials in which the 4-Methoxyphenylhydrazine hydrochloride **1** reacted with dimedone **2** in glacial acetic acid at room temperature for 2 hours and the reaction mixture continued under reflux for further 2.5 hours. The resulting tetrahydrocarbazole **3** was in a convenient yield 22.5% that was enough to obtain the starting material in a short time and submit it to the next step. The melting point of **3** was measured to record 235^oC that was too close to the reported melting point (240^oC).

N-benzoyl derivative **4** of the prepared tetrahydrocarbazole **3** was prepared by reacting **3** with 4-chlorobenzoyl chloride using 4-*N,N*-dimethylaminopyridine (DMAP) and trimethylamine (TEA) as mild base catalysts in dichloromethane (DCM) to afford the target product **4** in a quantitative yield after stirring at room temperature for 2 hours.

Tetrahydrocarbazole derivatives **5a,b** were prepared by reacting the starting tetrahydrocarbazole **3** with 4-chlorobenzyl bromide and 4-chlorophenylsulfonyl chloride in anhydrous dimethylformamide (DMF) using sodium hydride as base catalyst to give the corresponding *N*-benzyltetrahydrocarbazole **5a** and *N*-phenylsulfonyltetrahydrocarbazole **5b** in a quantitative yield after stirring for 1 hour at room temperature.

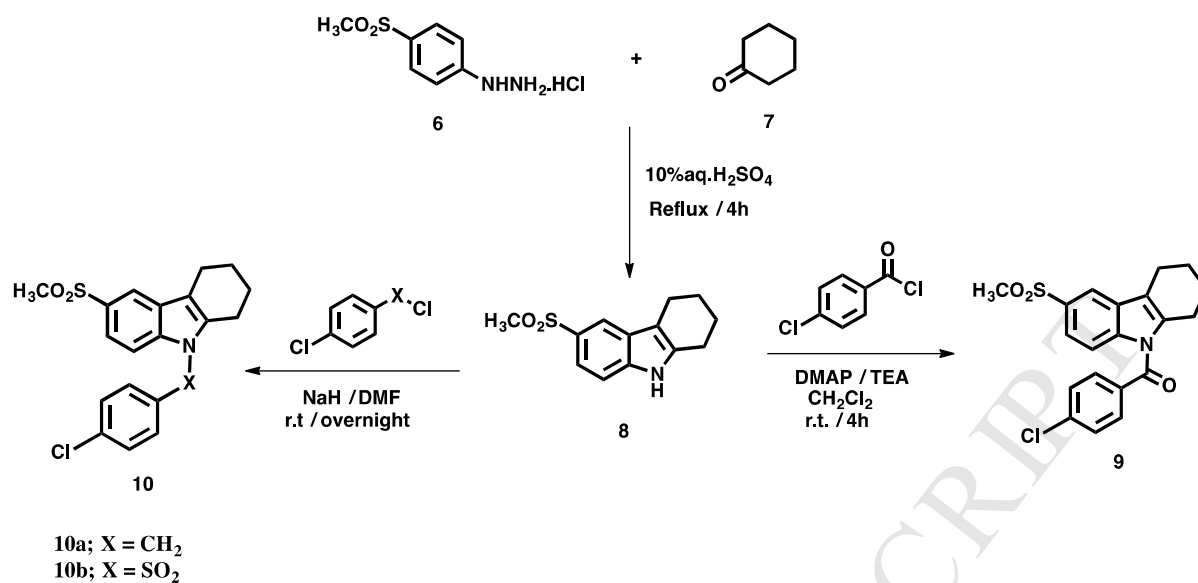


Scheme 1. Synthesis of target COX-2 inhibitors **4** and **5**.

The starting 6-(Methylsulfonyl)-2,3,4,9-tetrahydro-1*H*-carbazole **8** was reported previously by Mittapalli et al[29] in 2012 without any published spectral data about the compound but it has been mentioned that it was prepared by one-step reaction of cyclohexanone with 4-Methylsulfonylphenyl hydrazine hydrochloride in refluxing acetic acid overnight. It is worthy to mention that we adopted a different laboratory friendly method and kind of green chemistry as well; in which the ketone **7** and phenyl hydrazine HCl **6** were dissolved in hot 10% aqueous sulfuric acid and left under reflux for only 4 hours as shown in **scheme 2** to afford the target tetrahydrocarbazole **8** as a heavy microcrystalline precipitate separated from the reaction mixture in 76% yield. The product was confirmed by IR, ¹H-NMR, ¹³C-NMR, Mass spectrometry and microanalysis.

Tetrahydrocarbazole **8** reacted with 4-chlorobenzoyl chloride in DCM in the presence of TEA and DMAP at room temperature for 4 hours to afford the product **9** in 53% yield. The starting material was not completely converted into the corresponding product but it was easy to purify the product by fractional crystallization in boiling methanol.

Reaction of tetrahydrocarbazole **8** with both 4-chlorobenzyl chloride and 4-chlorophenylsulfonyl chloride went efficiently and completely in anhydrous DMF in the presence of NaH at room temperature and stirring overnight to afford the corresponding *N*-benzyl derivative **10a** and *N*-phenylsulfonyl derivative **10b** in 68% and 81% yields respectively.

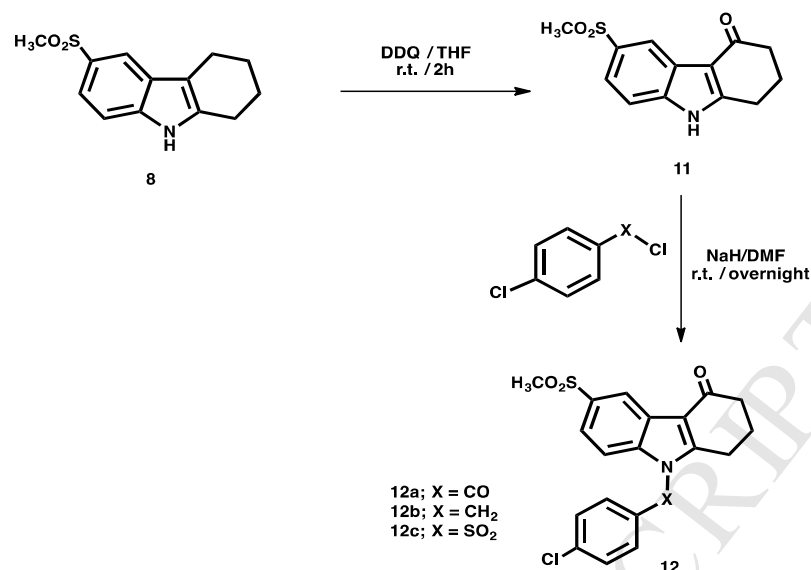


Scheme 2. Synthesis of target selective COX-2 inhibitors **9** and **10**.

The target compounds **12** were prepared as shown in **scheme 3** in which 6-(Methylsulfonyl)-2,3,4,9-tetrahydro-1*H*-carbazole **8** was exposed to 2 equivalents of DDQ in aqueous tetrahydrofuran (THF) that is an oxidizing agent very specific for the type of oxidation we aimed to achieve[30]. The reaction gave immediately after few seconds of stirring at room temperature a white fibrous crystalline precipitate of 6-(Methylsulfonyl)-1,2,3,9-tetrahydro-4*H*-carbazol-4-one **11** and the reaction was continued stirring at room temperature for further 2 hours to get it complete. The product was used for the next step without further crystallization.

Using NaH as a base catalyst in anhydrous DMF was chosen to prepare the *N*-benzoyl, *N*-benzyl and *N*-phenylsulfonyl **12a**, **12b** and **12c** derivatives respectively. Interestingly, *N*-benzoyl-tetrahydrocarbazole-4-one **11** couldn't be obtained efficiently applying the previous reaction conditions that were used to prepare the *N*-benzoyl derivatives **4** and **9**. This is attributed to the reaction that was not complete the same as **9** but couldn't be purified by fractional crystallization and the TLC check showed a lower conversion of the starting tetrahydrocarbazole **11** into the target product **12a**.

All the final products **4**, **9** and **12** were confirmed by IR, ¹H-NMR, ¹³C-NMR, Mass spectrometry and microanalysis.



Scheme 3. Synthesis of target selective COX-2 inhibitors 12.

2.2. Biological activity:

2.2.1. Human COX-1 and COX-2 enzymatic assay

The tetrahydrocarbazoles **4**, **5**, **9**, **10** and **12** generated for exploring it as selective COX-2 inhibitors, were tested against both hCOX-1 and hCOX-2 isoenzymes as an *in vitro* preliminary study to investigate the potential of the compounds to inhibit selectively COX-2 using Indomethacin and Celecoxib as standard non-selective and selective inhibitors respectively.

The results shown in (Table 1) revealed the discovery of new analogs of indomethacin **10a** ($\text{IC}_{50} = 0.28$), **10b** ($\text{IC}_{50} = 0.34$) and **12a** ($\text{IC}_{50} = 0.23$) with potential COX-2 inhibition and comparable activities to Celecoxib ($0.3 \mu\text{mol}$). It is worthy to emphasize that 9-(4-chlorobenzoyl)-6-(methylsulfonyl)-1,2,3,9-tetrahydro-4H-carbazol-4-one **12a** performed 1.3 times more potency than Celecoxib against COX-2 and 400 times less potency ($\text{IC}_{50} = 104 \mu\text{mol}$) than Indomethacin ($\text{IC}_{50} = 0.26 \mu\text{mol}$) against COX-1 to infer a future candidate with impressively selective COX-2 inhibition activity. Moreover, the superior selectivity ratio of **12a** (452.1739) reflected the outstanding selective COX-2 inhibition activity and made the minimal gastric irritation side effect be greatly expected.

Interestingly, the 6-methoxy derivatives of the generated tetrahydrocarbazoles **4** ($\text{IC}_{50} = 0.97 \mu\text{mol}$), **5a** ($\text{IC}_{50} = 0.91 \mu\text{mol}$), and **5b** ($\text{IC}_{50} = 0.88 \mu\text{mol}$) showed more potent inhibition activity against COX-2 than indomethacin ($\text{IC}_{50} = 2.63 \mu\text{mol}$) by 3.23, 3.03, and 2.93 times respectively but less potent than Celecoxib against the same enzyme. Thus, there might be another mechanism by which the new tetrahydrocarbazoles **4,5** inhibited COX-2 other than the interaction with the hydrophilic side pocket like what happens in case of Celecoxib and the formation of salt bridge with Arg120 like what happens in case of indomethacin. Moreover, the impressive decrease in the inhibition activity of the corresponding analog **4** to indomethacin against COX-1 ($\text{IC}_{50} = 201 \mu\text{mol}$) made us conclude that our hypothesis regarding the design of ring-extended analogs of indomethacin was successfully verified. Thus, 9-(4-Chlorobenzoyl)-6-methoxy-2,2-dimethyl-1,2,3,9-tetrahydro-

4*H*-carbazol-4-one **4** is expected to perform more anti-inflammatory activity with much less gastric irritation side effect than the original indomethacin prototype.

Table 1. *In Vitro* hCOX-2 and hCOX-1 enzymes inhibitory activities of compounds 4, 5, 9, 10, and 12.

Test compound	COX-2 IC ₅₀ ^a (μmol)	COX-1 IC ₅₀ ^a (μmol)	Approximate selectivity ratio ^b COX-1/ COX-2
Indomethacin	2.63±0.0021	0.26±0.0043	0.098859
Celecoxib	0.3±0.0015	100±3.45	333.3333
4	0.97±0.0093	201±5.44	207.2165
5a	0.91±0.0082	178±4.55	195.6044
5b	0.88±0.0074	167±3.76	189.7727
9	0.81±0.0063	152±4.67	187.6543
10a	0.28±0.0043	118±3.93	421.4286
10b	0.34±0.0024	120±1.06	352.9412
12a	0.23±0.0034	104±4.54	452.1739
12b	0.58±0.0051	137±2.97	236.2069
12c	0.79±0.0072	145±3.88	183.5443

^aThe *in vitro* test compound concentration required to produce 50% inhibition of COX-1 or COX-2.

^bThe *in vitro* COX-2 selectivity ratio (COX-1 IC₅₀/COX-2 IC₅₀).

2.2.2. Carrageenan-induced rat paw edema

The synthesized analogs, 6-methoxytetrahydrocarbazoles **4**, **5** and 6-methylsulfonyltetrahydrocarbazoles **9**, **10**, and **12** were subjected to *in vivo* testing implementing Carrageenan-induced rat paw edema bioassay.

According to the data results expressed in %protection; listed in (Table 2), 6-methylsulfonyltetrahydrocarbazole **12a** (88.05668%) showed the best %protection against Carrageenan-induced paw edema in rats to be more than that was shown by indomethacin (74.49%) and comparable to that of Celecoxib (96.73%). Interestingly, the results went aligned with what we got from the *in vitro* testing against hCOX-1 and hCOX-2 enzymatic assay (Table 1) except for the Celecoxib that gave %protection more than **12a**. It is important to emphasize that the extremely high %protection from the inflammation, sometimes, is not in the favor of the tested compound to be a future anti-inflammatory agent because it might magnify the cardiovascular (CVS) side effects of selective COX-2 inhibitors as a common class effect and vice versa. Thus, it is expected for compound **12a** to be potentially selective COX-2 inhibitor with less CVS problems than that reported for Celecoxib. Other indomethacin analogs exhibited higher %protection (Table 2) than the indomethacin prototype, to prove the significant improvement in the anti-inflammatory potential of the corresponding ring-extended new candidates.

Table 2. Effects of the tested compounds 4,5,9,10, and 12 on Carrageenan-induced rat paw edema (mL), percentage protection and activity relative to indomethacin.

Test compounds	Increase in paw edema (mL) ± SEM ^{a,b}	% Protection
Control	0.988±0.0006	0
Indomethacin	0.25±0.0005	74.49±4.44

Celecoxib	0.291±0.00053	96.73±3.44
4	0.201±0.00024	79.65587±2.43
5a	0.194±0.00015	80.36437±3.54
5b	0.191±0.00026	80.66802±4.45
9	0.188±0.00037	80.97166±3.66
10a	0.123±0.00022	87.55061±2.35
10b	0.145±0.00034	85.32389±2.63
12a	0.118±0.00043	88.05668±4.34
12b	0.167±0.00015	83.09717±3.74
12c	0.179±0.00026	81.88259±4.55

^a SEM denoted the standard error of the mean.

^b All data are significantly different from control (P < 0.001).

2.2.3. Estimation of plasma prostaglandin E2 (PGE2)

Measuring the percentage plasma levels of prostaglandin E2 (PGE2) after treating the animals with the COX-2 inhibitors using Indomethacin and Celecoxib as standard inhibitors is one of the important parameters to assess the anti-inflammatory potencies of the COX-2 inhibitors *in vivo*. The results are shown in (Table 3), revealed the highest anti-inflammatory potency with compound **12a** to record %inhibition of plasma PGE2 = 91.29 to be of superior PGE2-diminishing activity to Celecoxib ((%inhibition = 77.25). All other inhibitors performed higher potential as PGE2 lowering agents than Celecoxib but quite lower than indomethacin (%inhibition = 98.29) especially for 6-methoxy congeners **4**, **5a** and **5b** (80.24%, 81.16% and 82.16% respectively).

Table 3. Anti-inflammatory potencies of indomethacin analogs 4,5,9, and 10, and 12 (%inhibition of plasma PGE2).

Test compound	Inhibition of plasma PGE2 [%]±SEM ^{a,b}
Indomethacin	98.29±7.5
Celecoxib	77.25±6.6
4	80.24±3.5
5a	81.16±4.4
5b	82.16±3.6
9	83.19±2.5
10a	89.43±3.8
10b	88.20±4.9
12a	91.29±4.7
12b	86.39±5.8
12c	84.11±4.7

^a SEM denoted the standard error of the mean.

^b All data are significantly different from control (P < 0.001).

2.2.4. Human, Rat, and Dog Microsomal COX Assays

The resulted indomethacin analogs **4**, **5**, **9**, **10** and **12** in this study were tested against human, dog and rat microsomal COXs to evaluate their nanomolar inhibition activities using Celecoxib as standard inhibitor. As shown in (Table 4), compound **12a** ($IC_{50} = 23$ nM) was the most potential human COX inhibitor and it performed lower potential activity ($IC_{50} = 34$ nM, and 48 nM) against dog and rat microsomal COX respectively. Additionally, Compound **12a** and all the other indomethacin analogs **4**, **5**, **9**, and **10** were significantly and in a selective fashion in the favor of human microsomal COX to be more potent against human, dog and rat microsomal COX than the standard inhibitor ($IC_{50} = 89$ nM, 112 nM and 132 nM) respectively.

Table 4. Effect of indomethacin analogs 4,5,9,10, and 12 on Human, Dog, and Rat Microsomal COX Activities

Test compound	IC ₅₀ nM		
	Human	Dog	Rat
Celecoxib	89±5.6	112±9.7	132±8.5
4	50±3.6	80±5.5	141±9.6
5a	44±3.8	77±4.7	132±8.8
5b	41±2.7	61±8.6	128±9.7
9	38±1.9	56±4.4	116±7.8
10a	27±2.7	39±1.6	56±4.7
10b	28±1.6	40±2.5	79±3.6
12a	23±1.6	34±1.7	48±2.6
12b	33±2.7	45±3.4	93±5.7
12c	34±1.8	53±3.3	104±6.9

Values were calculated from the mean values of data from three separate experiments and presented as mean value ± SEM.

All results are significantly different from control values at $p \leq 0.005$.

2.2.5. Cotton pellet-induced granuloma bioassay

New indomethacin analogs **4**, **5**, **9**, **10**, and **12** were subjected to Cotton pellet-induced rat granuloma bioassay and the inhibition activities are listed in (Table 5) expressed in ED_{50} . Consistently, 6-methylsulfonyltetrahydrocarbazole-4-one **12a** ($ED_{50} = 12.38$ μ mol) performed the highest anti-inflammatory activity as it inhibited the Cotton pellet-induced rat granuloma 0.75 times of indomethacin ($ED_{50} = 9.568$ μ mol) and 6.95 times of Celecoxib ($ED_{50} = 86.11$ μ mol) though the comparable activity of **12a** to Celecoxib in the enzymatic assay (Table 1). This might be attributed to the metabolic enzymes effect on compound **12a** that led to more active metabolite. Or, the bioavailability of **12a** might have played a significant role in such *in vivo* bioassay results.

The other tetrahydrocarbazoles **4**, **5**, **9**, **10**, and **12b,c** gave significantly higher inhibition activities than Celecoxib (Table 5). Based on the ED_{50} recorded for the new analogs, we could conclude that we have interesting compounds, combine between the potential anti-inflammatory (Table 5) and selective activities (Table 1), excel the anti-inflammatory profile of both indomethacin and Celecoxib.

Table 5. Anti-inflammatory potencies of indomethacin analogs 4,5,9,10, and 12 (inhibition of Cotton pellet-induced granuloma in ED₅₀, μ mol).

Test compounds	ED ₅₀ (μ mol)
Indomethacin	9.568 \pm 0.87
Celecoxib	86.11 \pm 1.23
4	28.27 \pm 1.90
5a	17.27 \pm 1.56
5b	26.88 \pm 1.36
9	25.67 \pm 1.67
10a	14,56 \pm 0.99
10b	18.67 \pm 1.34
12a	12.38\pm0.89
12b	19.20 \pm 1.22
12c	22.33 \pm 1.34

2.2.6. Ulcerogenic effects

The percentage of ulcerogenic activity of indomethacin analogs **4**, **5**, **9**, **10** and **12** were calculated after exposure of the experimental animals to the tested compounds using indomethacin and Celecoxib as standard drugs. According to the data recorded for each compound in (Table 6), compound **12a** exhibited the lowest ulcerogenic activity (3.28%) to be 30.48 times safer than indomethacin (100%) and 0.64 times as safe as Celecoxib (2.11%). All the other analogs showed significant reduction in the ulcerogenic activity when compared to indomethacin and the maximum percentage of ulceration was for 6-methoxytetrahydrocarbazole **5b** (20.12%). This indicates that the safety margin of the new analogs became impressively wider than the original prototype to reflect the real existence of compounds with potential anti-inflammatory activity (Tables 2, 3, 5) and greatly lower ulcerogenic activity, specifically those are 6-methylsulfonylphenyltetrahydrocarbazole derivatives **10a,b** and **12a,b** though it didn't excel the Celecoxib's safety against ulcerogenic activity.

Table 6. The percentage ulcerogenic activity^a of Indomethacin analogs 4, 5, 9, 10, and 12

Test compounds	% Ulceration
Indomethacin	100 \pm
Celecoxib	2.11 \pm 0.23
4	13.18 \pm 0.23
5a	11.20 \pm 0.12
5b	20.12 \pm 0.33
9	12.45 \pm 0.24
10a	4.48 \pm 0.54
10b	2.90 \pm 0.63

12a	3.28±0.12
12b	5.40±0.52
12c	11.29±0.45

^a All data (tested compounds, indomethacin and Celecoxib) were significantly different from control ($P < 0.001$)

2.3. Molecular docking studies:

Molecular docking was done in order to predict the molecular orientation of the synthesized compounds into the COX-2 binding site and to interpret the biological activities results. In addition to the docking score, some other parameters such as; the lipophilic contribution score, clash score and conformation entropy score were computed to find out a suitable correlation to the biological results (**Table 7**).

Table 7. Molecular docking results of the synthesized compounds using Leadit 2.1.2

Test compound	Docking score Kcal/mol	Lipo score	Clash score	Rot Score
4	-18.98	-16.85	10.34	4.20
5a	-15.60	-17.31	12.00	4.20
5b	-21.85	-16.21	10.78	1.40
9	-23.92	-16.65	9.34	1.40
10a	-23.36	-17.14	8.90	4.20
10b	-23.40	-15.21	8.36	4.20
12a	-30.78	-15.41	7.21	1.40
12b	-23.05	-15.85	8.65	4.20
12c	-23.95	-16.75	9.28	4.20
Indomethacin	-31.23	-14.66	7.03	4.20
Celecoxib	-35.41	-15.59	9.67	4.20

Docking score (Kcal/mol): free binding energy value. *Lipo score:* Lipophilic contribution score.
Clash score: Contribution of the clash penalty. *Rot score:* Ligand conformational entropy score

Computing of the docking score was able to compare the binding free energies of the synthesized compounds and comparing them to both Indomethacin and Celecoxib. Compound **12a** showed the best docking score (-30.78 kcal/mol) which is very close to that of both Indomethacin and Celecoxib (-31.23 and -35.41 kcal/mol respectively). The lipophilic contribution score values (Lipo score) listed in (**Table 7**) inferred its insignificant effect. The clash penalty score should be a small value to avoid the steric repulsion of the generated conformations. It was observed that compound **12a** and Indomethacin shared the common feature of low clash score 7.21 and 7.03 respectively. The Ligand conformational entropy score (Rot score) is implemented in Leadit software to compute the effect of the degree of freedom of the flexible compounds that can affect their rotations and orientations. It is much better to have a neglected or a small value for this score. From all the docked compounds, derivatives **5b**, **9**, and **12a** only showed the lowest value (1.40) for the Ligand conformational entropy score which confirmed their stability in the active site. All compounds featured a common orientation

mode in which the p-chlorobenzyl or p-chlorobenzoyl moieties were superimposed to that of Indomethacin. The docking scores illustrated in (Table 7) were proportional to the inhibitory IC_{50} values of COX-2 (Figure 4).

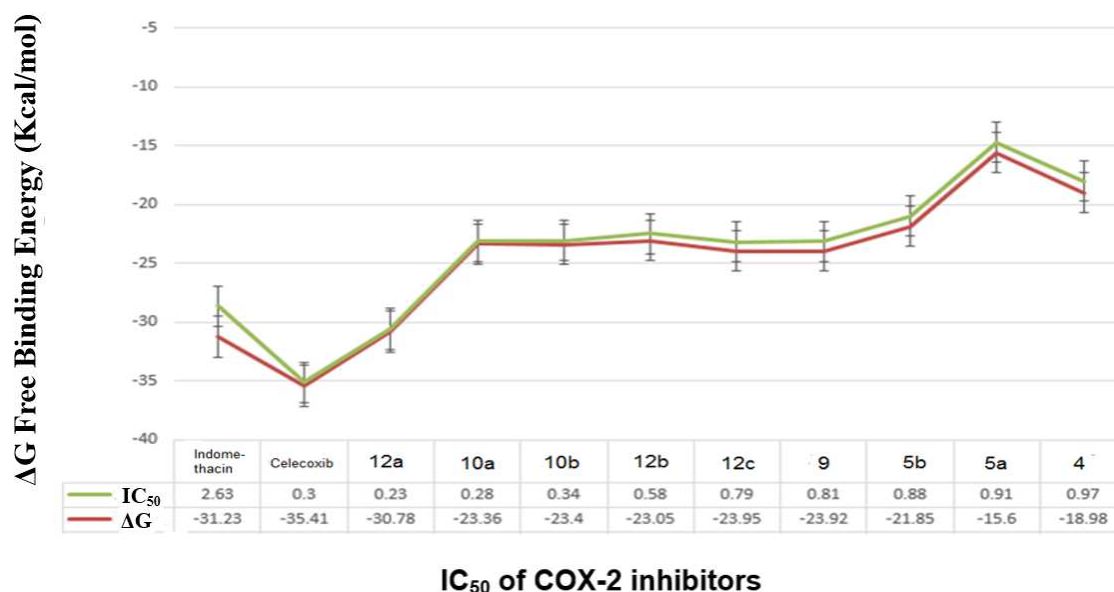


Fig. 4. Correlation between the docking scores and the IC_{50} of new COX-2 inhibitors.

Celecoxib is a selective COX-2 inhibitor which has a unique binding mode in a polar side pocket found in COX-2 isozyme. The reason is correlated to its SO_2-NH_2 group that has the ability to form many interactions with residues found in this side pocket such as Arg499, Ser339, Leu338, and Gln178 (Figure 5A). The crystal structure of the most active compound **12a** in complex with COX-2 that was subjected to MD simulations was used to inspect the interactions of this compound with these specified residues. Upon visualization of the formed interactions we found that the methyl sulfonyl group CH_3-SO_2 of this compound has a hydrogen bond with Arg499 and Ser339 (Figure 5B). It was clear that the impact of the $-NH_2$ in SO_2-NH_2 side chain of Celecoxib is higher than the CH_3- group in SO_2-CH_3 in our compound and that may be a start point for an optimization process in the future for our lead compound.

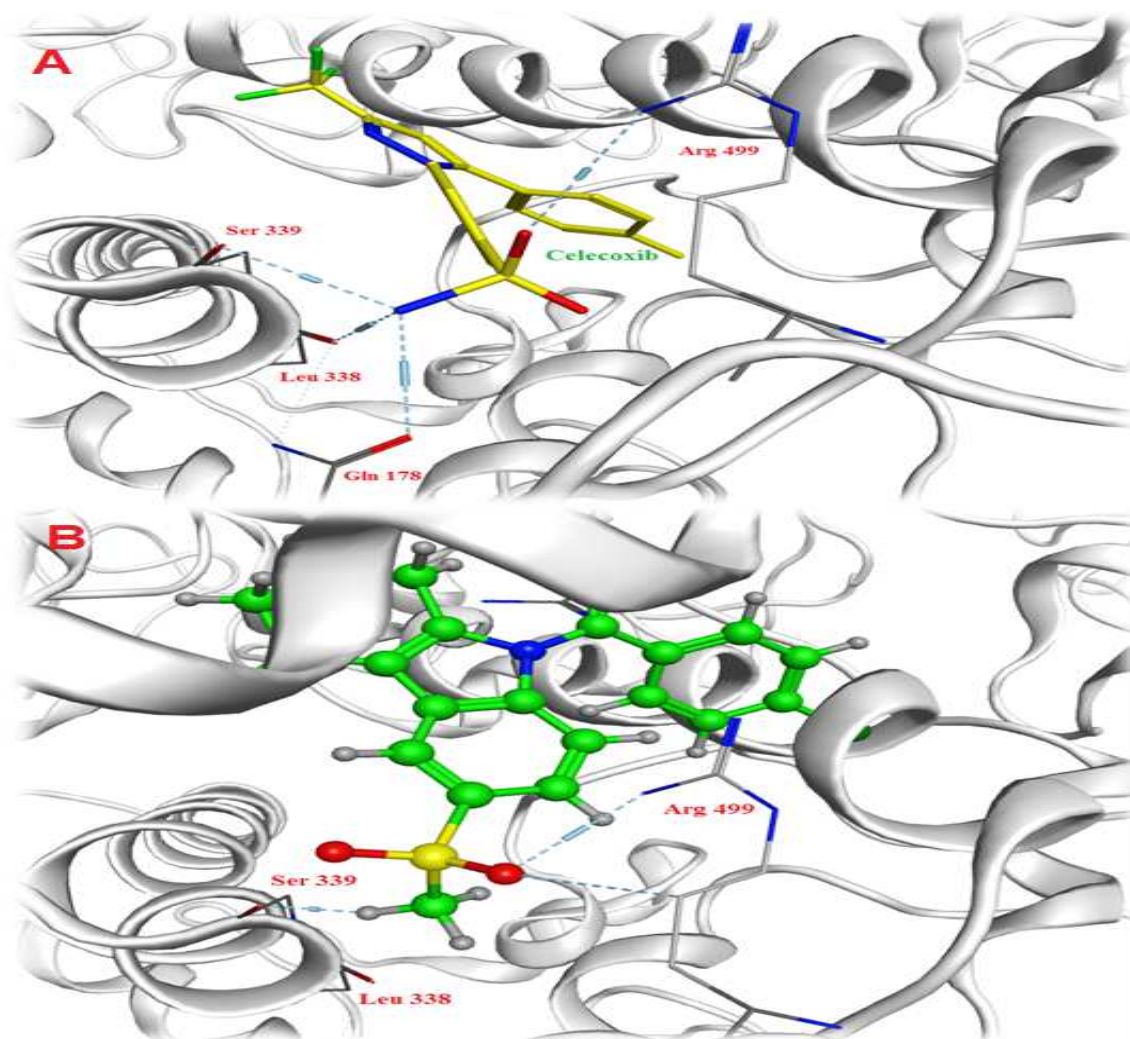


Fig. 5. A) Best binding mode of Celecoxib to COX-2. B) Best binding pose of (12a) into COX-2 binding site. The binding site is represented as cartoon in grey color. Celecoxib was built as stick form (Yellow color). Compound (12a) was built as ball and stick (Green color). Hydrogen bonds of ligand atoms with the amino acid residues of binding site are in light blue dotted lines.

The docking results of compounds **4**, **5a** and **5b** with the lowest IC_{50} values in the *in vitro* COX-2 inhibitory assay revealed that these compounds showed also low predicted docking score; -18.98, -15.60, and -21.85 kcal/mol respectively. In addition, the clash contribution score of these compounds (10.34, 12.00, and 10.78 respectively) was higher than the most active compound **12a** (7.21).

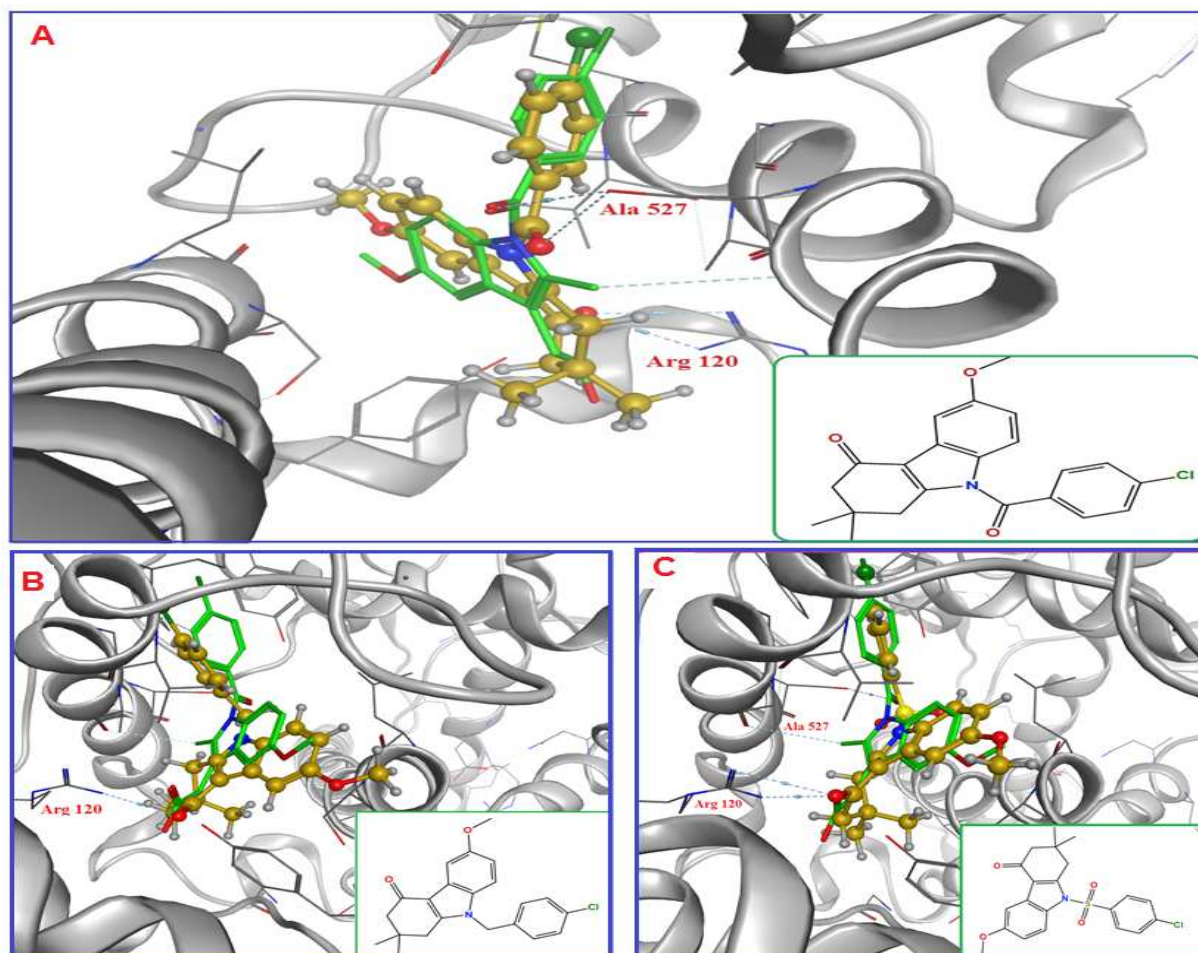


Fig. 6. The best pose resulted from the docking of A) compound (4), B) compound (5a) and C) compound (5b) into COX-2 binding site. The binding site is represented in cartoon (grey color), Indomethacin is in stick form (green color). The synthesized derivatives are in ball and stick form (golden color). Hydrogen bonds of ligand atoms with the amino acid residues of binding site are in light blue dotted lines.

Compound **4** showed the same orientation as indomethacin (Fig. 6A), its CO of the cyclohexyl ring interacts via hydrogen bond formation with Arg120 while its benzoyl-CO showed hydrogen bond with Ala527. The same interaction of the cyclohexane-CO was also observed in both **5a** (Fig. 6B) and **5b** (Fig. 6C).

2.4. Generalized Born Poisson Boltzmann (MM/GBVI)

Molecular mechanics can be used to compute the non-bonded interactions. Generalized Born Poisson Boltzmann (MM/GBVI) was used to calculate the binding strengths of the non-bonded interactions in kcal/mol (Table 8). It is used to estimate the relative binding strengths via estimation of the change of enthalpy takes place upon binding. It was clear that compounds **10a**, **12b**, **10b**, **5b**, showed -21.13 kcal/mol, -18.44 kcal/mol, -15.78 kcal/mol, and -13.78 kcal/mol respectively. When these values were compared to that of Celecoxib (-16.37 kcal/mol), it seemed that they were close to each other in this kind of interactions. On the other hand, compound **5b** showed -26.90 kcal/mol and was the only compound to be close to Indomethacin's value (-25.61 kcal/mol).

Table 8. Some calculated parameters for the synthesized compounds

Test compound	TPSA	ClogP	MM/GBVI Kcal/mol	Affinity pki
4	48.30	5.14	-11.94	10.68
5a	31.23	5.77	-26.70	9.88
5b	48.30	5.14	-13.78	9.26
9	56.14	4.26	-11.11	9.46
10a	39.07	4.89	-21.13	9.00
10b	73.21	3.81	-15.78	9.56
12a	73.21	3.90	-12.36	10.67
12b	56.14	4.53	-18.44	10.16
12c	90.28	3.45	-15.75	10.46
Indomethacin	71.36	2.59	-25.61	10.21
Celecoxib	77.98	3.82	-16.37	11.47

TPSA: Topological Polar Surface Area. *ClogP*: calculated logarithm of compound partition coefficient. *MM/GBVI*: Generalized Born Poisson Boltzmann

All compounds had a ClogP value within the accepted range of the drug-like properties. The affinity pki value of Celecoxib was the highest (11.47). Compounds **4** and **12a** showed the top two values of pki; 10.68 and 10.67 respectively.

2.5. Topological Polar Surface Area (TPSA)

The limited number of the synthesized compounds (only 9 compounds) made it difficult to perform 3D QSAR study in order to find out the descriptors to which the biological data may be correlated. Instead, another 2D descriptor can be used to measure the polar surface area. TPSA, was calculated (**Table 8**). It measures the polar surface area that can be useful when predicting an agent's bioavailability. Compounds with low values (i.e., <75) were identified to be associated with various side effects. According to the results, Celecoxib had a value of 77.98 which confirmed its high polar surface area and COX-2 selectivity toward binding to the polar cavity found in COX-2. It was clear that Compound **12c** was the highest value (90.28). Compounds **10b**, and **12a** showed the same TPSA (73.21). Compounds **9** and **12b** had the same as well (56.14) and finally, both compounds **4** and **5b** showed similar TPSA (48.30). The inhibitors' IC₅₀ values for COX-2 were proportional to TPSA values (**Figure 7**).

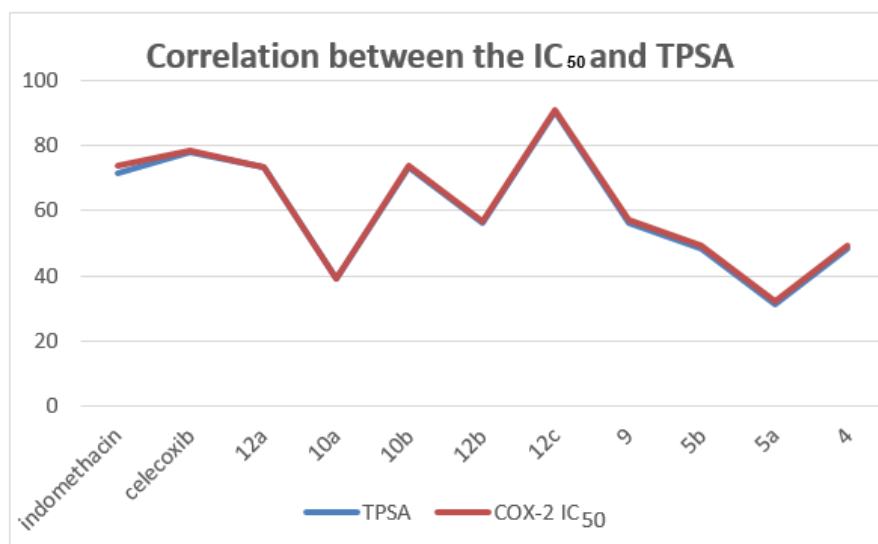


Fig. 7. Correlation between IC₅₀ of new COX-2 inhibitors and TPSA

2.6. Molecular Dynamic simulation.

Molecular dynamic relaxation was done to validate the stability of the most active compound **12a** within the active site of COX-2. Time of the dynamics process was computed over 10000 picoseconds (ps) period of time, the potential energy of the atomic system in kcal/mol, and the kinetic energy of atoms in kcal/mol. The simulations were done in two steps. First, NAMD was obtained from university of Illinois (www.ks.uiuc.edu/research/namd.) The simulations' running started and after 10000 ps, the trajectory file was imported and analyzed. Here, the potential energy (Kcal/mol) showed a sharp increase with time then a decline in which the steady state was not observed (**Figure 8A**). Regarding the kinetic energy (Kcal/mol) of the atomic system, it did not give an ideal curve where the start was low kinetic value and a steady state was absent as well (**Figure 8B**). The ligand-COX-2 complex resulted from NAMD MD was used in the second step that was conducted by MOE molecular dynamic simulations. Here, the potential energy showed almost a typical mode of minimization where the energy increased with time until a steady state was reached (**Figure 9A**). The kinetic energy of the **12a**-COX-2 complex started by a scattered mode of atoms followed by a steady state as well (**Figure 9B**). The ligand-COX 2 complex now can be considered to be in a stable form where we can study the effects of MD on the interactions of the most active compound. The main difference between the potential energy profile and that of kinetic energy profile of **12a**-COX-2 complex can be observed in the figures where the equilibrium was reached in case of potential energy at 15 ps (**Figure 9A**) while the oscillations in case of the kinetic energy reached the equilibrium at 20 ps (**Figure 9B**) which is a very small difference.

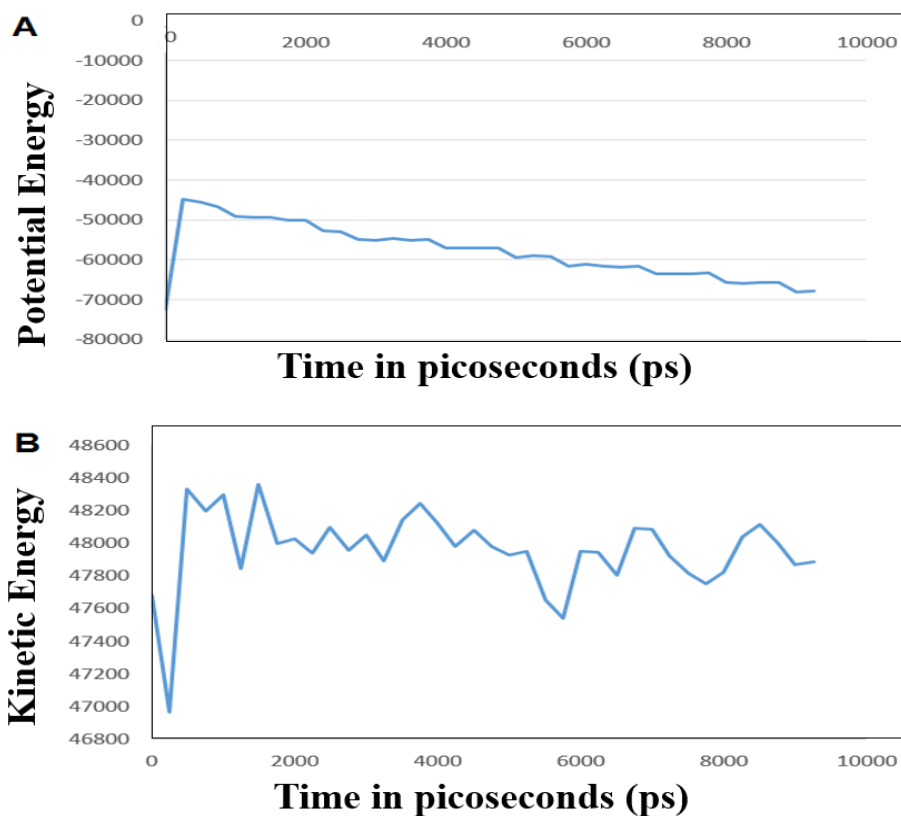


Fig. 8. NAMD showing the relation between both the A) Potential energy, B) Kinetic energy and time

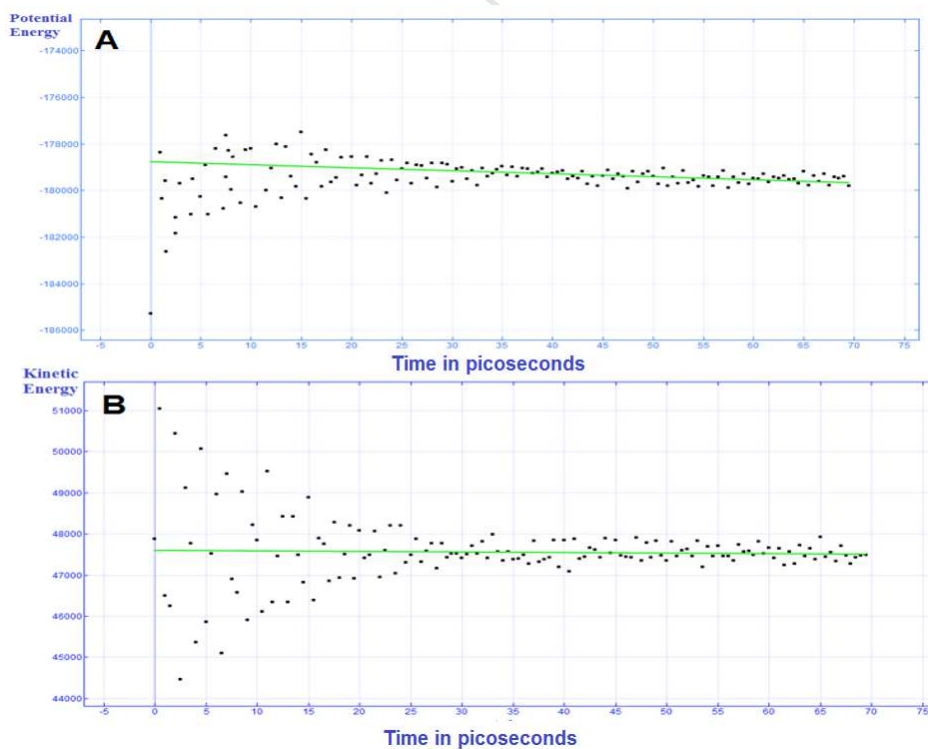


Fig. 9. MD simulations represents the points of oscillations of the complex (12a-COX-2) atoms showing: A) Potential energy (Kcal/mol) and B) Kinetic energy (Kcal/mol) profile resulted from MD simulation.

3. Conclusion:

The present study introduced a new perspective and novel strategy that hasn't been discussed or even suggested before for the improvement of the selectivity of indomethacin against COX-2 isoenzyme. The new strategy involved i) ring extension, ii) Deletion of carboxylic acid and iii) introduction of methylsulfonyl group to reduce the possibility of COX-1 inhibition by the new candidates and increase the opportunity of COX-2 inhibition as well. The biological activity data profile of the generated ring-extended analogs verified the success of the strategy provided, that confirmed the efficacy of the analogs as anti-inflammatory agents against COX-2 in a potentially selective fashion excelling the selectivity ratio of Celecoxib with 6-methylsulfonylphenyltetrahydrocarbazoles **10a** and **12a**. In addition, all the new analogs showed high safety margin against gastric ulceration in comparison to indomethacin and the safety was so close to Celecoxib with 6-methylsulfonylphenyltetrahydrocarbazoles **10a,b** and **12a,b** to confirm the necessity of methylsulfonyl group in improving the selectivity of new inhibitors against COX-2. The COX-1 and COX-2 inhibition potencies of 6-Methoxytetrahydrocarbazoles **4** and **5** proved the significant effect of ring extension and deletion of carboxylic acid on increasing the selectivity ratio and COX-2 inhibition potency as well. The high PGE2 lowering potential of **12a** with the other anti-inflammatory descriptors data profile highlights this analog as a very potential and selective COX-2 inhibitor. The docking scores obtained for the new candidates confirmed the potential selectivity of **12a** by having the highest binding affinity. The molecular dynamic study indicated the stability of **12a** into the catalytic binding site. Conclusively, the study provided the field with new class of potentially selective COX-2 inhibitors is superior to Celecoxib based on the *in vitro*, *in vivo* biological data profiling recorded. It is worthy to mention that the current investigation paved the road for the researchers including us to elaborate in the near future other new classes of COX-2 inhibitors beyond the diarylsulfonamides class applying the new strategy that is introduced by us.

4. Experimental:

3.1. Chemistry

Melting points were determined on digital Gallen-Kamp MFB- 595 instrument using open capillary tubes and are uncorrected. IR spectra were recorded as potassium bromide discs on Shimadzu FT-IR 440 spectrometer. ¹H NMR spectra were recorded on Bruker spectrophotometer at 300 MHz in DMSO-*d*₆; values (δ) are given in parts per million (ppm) downfield from tetramethylsilane (TMS) as internal reference. ¹³C NMR spectra were recorded using the same spectrophotometer that used for recording ¹H NMR. Mass spectra were recorded on Thermo Triple stage quadropole mass spectrometer. The elemental analyses were performed at the Microanalytical Center, Cairo University, Cairo, Egypt. Reactions were followed up by thin layer chromatography (TLC) using Merck Silica gel/TLC cards with fluorescent indicator UV254 using Hexane:Ethyl acetate (EtOAc) 1:1 as the eluting system and the spots were visualized using Spectroline E series dual wavelength UV lamp at λ=254 nm.

Synthesis of 6-methoxy-2,2-dimethyl-1,2,3,9-tetrahydro-4H-carbazol-4-one (3)

A mixture of 4-methoxyphenylhydrazine HCl (3 mmol, 0.524 g) and dimedone (3 mmol, 0.42 g) were suspended in acetic acid glacial (15 mL) and left stirring at room temperature for 2 hours. The temperature of the reaction mixture was raised to reflux for 2.5 hours. The solvent was evaporated under reduced pressure to give dark brown sticky residue. The brown residue was subjected to column chromatography and eluted with Hexane: EtOAc 1:1 to give beige powder of the title compound in a pure form.

Yield: 22.5%, m.p.: 235 °C. IR (KBr) $\nu_{\max}/\text{cm}^{-1}$: 3172 (NH), 1616 (CO). ^1H NMR (DMSO- d_6 , 300 MHz): δ 1.08 (s, 6H, 2,2-di-CH₃), 2.31 (s, 2H, 3-H), 2.82 (s, 2H, 1-H), 3.76 (s, 3H, CH₃O) 6.80 (d, 1H, 7-H), 7.29 (d, 1H, 8-H), 7.45 (s, 1H, 5-H), 11.65 (s, 1H, NH).

Synthesis of 9-(4-Chlorobenzoyl)-6-methoxy-2,2-dimethyl-1,2,3,9-tetrahydro-4H-carbazol-4-one (4)

4-Chlorobenzoyl chloride (43 mg, 0.247 mmol) was added to a stirred suspension of tetrahydrocarbazole (50 mg, 0.205 mmol) in DCM (5 mL), DMAP (14.9 mg, 0.151 mmol) and TEA (0.15 mL) were then added. The reaction mixture got dissolved into solution after addition of the base catalysts, was left to stir at room temperature until the reaction got complete after 2 hours according to TLC test. The solvent was removed under reduced pressure and the resulting residue was washed several times with diethyl ether to give white needle crystals of the target compound with no need to further purification.

Yield: 40%, m.p.: 190-192 °C; IR (KBr) $\nu_{\max}/\text{cm}^{-1}$: 1696 (CO ketone), 1658 (CO amide). ^1H NMR (DMSO- d_6 , 300 MHz): δ 7.78 (d, $J=8.1$ Hz, 2H, 2,6-H), 7.67 (d, $J=8.2$ Hz, 2H, 3,5-H), 7.59 (s, 1-H, 5-H), 7.06 (d, $J=9.0$ Hz, 1H, 8-H) 6.83 (d, $J=9.0$ Hz, 1H, 7-H), 3.79 (s, 3H, CH₃O), 2.76 (s, 2H, 1-H), 2.42 (s, 2H, 3-H), 1.02 (s, 6H, 2,2-di-CH₃). ^{13}C NMR (DMSO- d_6 , 75 MHz): δ 27.86 (CH₃), 35.18 (C-2), 38.31 (C-1), 51.30 (C-3), 55.37 (CH₃O), 103.12, 112.75, 114.97, 115.05, 125.99, 129.15, 130.73, 131.71, 132.55, 138.64, 151.09, and 156.58 (Ar-C), 167.78 (CO-N), 194.31 (CO). MS LRMS (ESI): (calc) 381.11 (found) 382.15 (MH)⁺. Anal. Calcd for C₂₂H₂₀ClNO₃: C, 69.20; H, 5.28; N, 3.67. Found: C, 69.15; H, 5.44; N, 3.46.

Synthesis of 9-(4-Chlorobenzyl)-6-methoxy-2,2-dimethyl-1,2,3,9-tetrahydro-4H-carbazol-4-one (5a)

Tetrahydrocarbazole (50 mg, 0.205 mmol) was dissolved in dry DMF (1 mL) and the stirred solution was treated with NaH in oil dispersion 60% (17.8 mg, 0.266 mmol). The reaction mixture was stirred at room temperature for 10 min until the effervescence was ceased and then treated with 4-chlorobenzyl chloride (40 mg, 0.246 mmol), the stirring was continued at room temperature for 2 hours and poured onto ice-cold water. The resulting precipitate was filtered off and recrystallized from ethanol affording beige crystals of the title compound.

Yield: 54%; m.p.: 163-165 °C. IR (KBr) $\nu_{\max}/\text{cm}^{-1}$ 1640 (CO). ^1H NMR (DMSO- d_6 , 300 MHz): δ 7.52 (s, 1H, 5-H), 7.38 (d, $J=6.7$ Hz, 3H, 8-H, 2,6-H), 7.08 (d, $J=8.1$ Hz, 2H, 3,5-H), 6.80 (d, $J=8.8$ Hz, 1H, 7-H) 5.46 (s, 2H, 4-Cl-C₆H₄-CH₂), 3.77 (s, 3H, CH₃O), 2.84 (s, 2H), 2.35 (s, 2H), 1.07 (s, 6H, 2,2-di-CH₃). ^{13}C NMR (DMSO- d_6 , 75 MHz): δ 28.14 (CH₃), 34.93 (C-2), 35.23 (C-1), 45.57 (4-Cl-C₆H₄-CH₂), 51.53 (C-3), 55.31 (CH₃O), 102.62, 110.53, 111.40, 111.74, 124.94, 128.25, 128.69, 131.71, 131.99, 136.09, 151.40, and 155.71 (Ar-C), 192.14 (CO). MS LRMS (ESI): (calc) 367.13 (found) 368.10 (MH)⁺. Anal. Calcd for C₂₂H₂₂ClNO₂: C, 71.83; H, 6.03; N, 3.81. Found: C, 71.91; H, 6.20; N, 3.62

Synthesis of 9-[(4-Chlorophenyl(sulfonyl)]-6-methoxy-2,2-dimethyl-1,2,3,9-tetrahydro-4H-carbazol-4-one (5b)

Tetrahydrocarbazole (50 mg, 0.205 mmol) was dissolved in dry DMF (1 mL) and the stirred solution was treated with NaH in oil dispersion 60% (17.8 mg, 0.266 mmol). The reaction mixture was stirred at room temperature for 10 min until the effervescence was ceased and then treated with the appropriate 4-chlorophenylsulfonyl chloride (52 mg, 0.246 mmol), the stirring was continued at room temperature for 2 hours and poured onto ice-cold water. The resulting precipitate was filtered off and recrystallized from ethanol affording beige crystals of the title compound.

Yield: 62%; m.p.: 175 °C. IR (KBr) $\nu_{\max}/\text{cm}^{-1}$ 1656 (CO). ¹H NMR (DMSO-*d*₆, 300 MHz) δ 8.01 (t, *J*=8.4 Hz, 3H), 7.70 (d, *J*=8.3 Hz, 2H), 7.54 (s, 1H), 7.00 (d, *J*=9.3 Hz, 1H), 3.78 (s, 3H, CH₃O), 3.24 (s, 2H), 2.43 (s, 2H), 1.07 (s, 6H, 2,2-di-CH₃). ¹³C NMR (DMSO-*d*₆, 75 MHz): δ 27.75 (CH₃), 34.81 (C-2), 37.35 (C-1), 51.02 (C-3), 55.37 (CH₃O), 103.80, 113.80, 114.74, 126.31, 128.52, 129.49, 130.29, 135.82, 140.27, 150.55, and 157.19 (Ar-C), 194.21 (CO). MS LRMS (ESI): (calc) 417.08 (found) 418.12 (MH)⁺. Anal. Calcd for C₂₂H₂₂ClNO₂: C, 60.36; H, 4.82; N, 3.35. Found: C, 60.24; H, 4.67, N, 3.52

Synthesis of 6-(Methylsulfonyl)-2,3,4,9-tetrahydro-1H-carbazole (8)

A mixture of 4-methylsulfonylphenylhydrazine HCl (1.11 g, 5 mmol) and cyclohexanone (5 mmol, 0.50 mL) were heated at 80 °C for 5 min, 10% aq. H₂SO₄ (20 mL) was added to the solid mixture followed by vigorous stirring until complete dissolution. The temperature was raised to reflux; greenish-light brown solid crystalline product was separated out from the solution after 1 h of the reaction time, and the reflux continued to 4 hours. The reaction mixture was left to cool, diluted with 20 mL H₂O for more precipitation of the solid product, the solid product was filtered off, washed with H₂O (10 mL) and left to dry under vacuum. No further crystallization for purification was required and the product submitted directly to the next step.

Yield: 76%, m.p.: 169 °C, IR (KBr) $\nu_{\max}/\text{cm}^{-1}$ 3321 (NH), 1287 (CH₃SO₂). ¹H NMR (DMSO-*d*₆, 300 MHz) δ 11.28 (s, 1H, NH), 7.91 (s, 1H, 5-H), 7.51 (d, *J*=8.60 Hz, 1H, 7-H), 7.43 (d, *J*=8.4 Hz, 1H, 8-H), 3.12 (s, 1H, CH₃SO₂), 2.70 (m, 4H, 1,4-H), 1.83 (m, 4H, 2,3-H). ¹³C NMR (DMSO-*d*₆, 75 MHz): 20.30 (C-4), 22.57 (C-2,3), 22.68 (C-1), 44.68 (CH₃SO₂), 109.79, 110.90, 117.15, 118.45, 130.34 and 137.61, 137.78 (Ar-C). MS LRMS (ESI): (calc) 249.08 (found) 250.03 (MH)⁺. Anal. Calcd for C₁₂H₁₄N₂O₂S: C, 62.63; H, 6.06; N, 5.62. Found: C, 62.47; H, 6.23; N, 5.79.

Synthesis of 9-(4-Chlorobenzoyl)-6-methylsulfonyl-2,3,4,9-tetrahydro-1H-carbazole (9)

4-Chlorobenzoyl chloride (0.26 mL, 2.0 mmol) was added to a stirred suspension of tetrahydrocarbazole (249 mg, 1.0 mmol) in DCM (10 mL), DMAP (80 mg, 0.67 mmol) and TEA (0.75 mL) were then added. The reaction mixture got dissolved into solution after addition of the base catalysts, was left stirring at room temperature overnight. The solvent was removed under reduced pressure and the resulting residue was washed several times with diethyl ether. The solid residue recrystallized from ethanol to give off white microcrystalline product of the target compound.

Yield: 53%, m.p.: 207 °C, IR (KBr) $\nu_{\max}/\text{cm}^{-1}$ 1685 (CO), 1314 (CH_3SO_2). ^1H NMR (DMSO- d_6 , 300 MHz) δ 8.04 (s, 1H, 5-H), 7.70 (dd, $J=23.3, 8.5$ Hz, 5H, 2,6-H, 3,5-H, 7-H), 7.49 (d, $J=8.8$ Hz, 1H, 8-H), 3.21 (s, 3H, CH_3SO_2), 2.72 (t, 2H, 4-H), 2.47 (t, 2H, 1-H), 1.76 (m, 4H, 2,3-H). ^{13}C NMR (DMSO- d_6 , 75 MHz): 20.31 (C-4), 21.48 (C-3), 22.71 (C-2), 25.09 (C-1), 44.03 (CH_3SO_2), 114.69, 117.15, 117.43, 121.71, 129.05, 129.29, 131.26, 133.45, 135.06, 137.90, 138.17 (Ar-C), and 167.66 (CO-N). MS LRMS (ESI): (calc) 381.11 (found) 382.15 (MH)⁺. Anal. Calcd for $\text{C}_{12}\text{H}_{14}\text{N}_2\text{O}_2\text{S}$: C, 61.93; H, 4.68; N, 3.61. Found: C, 62.11; H, 4.81; N, 3.45.

Synthesis of 9-(4-Chlorobenzyl)-6-methylsulfonyl-2,3,4,9-tetrahydro-1H-carbazole (10a)

Tetrahydrocarbazole (249 mg, 1.0 mmol) was dissolved in dry DMF (3 mL) and the stirred solution was treated with NaH in oil dispersion 60% (52 mg, 1.3 mmol). The reaction mixture was stirred at room temperature for 1 hour and then treated with 4-chlorobenzyl chloride (193 mg, 1.2 mmol), the stirring was continued at room temperature overnight and then poured onto ice-cold water to give solid product. The solid product filtered off, dried under vacuum and suspended in ether with vigorous shaking then filtered off to give white powder of the corresponding *N*-benzyltetrahydrocarbazole in a pure form.

Yield: 68%, m.p.: 153 °C, IR (KBr) $\nu_{\max}/\text{cm}^{-1}$ 1302 (CH_3SO_2). ^1H NMR (DMSO- d_6 , 300 MHz) δ 8.00 (s, 1H, 5-H), 7.62 (d, $J=8.60$ Hz, 1H, 7-H), 7.59 (d, $J=8.60$ Hz, 1H, 8-H), 7.36 (dd, $J=8.1$ Hz, 2H, 2,6-H), 7.03 (dd, $J=8.1$ Hz, 2H, 3,5-H), 5.43 (s, 2H, 4-Cl-C₆H₄-CH₂), 3.15 (s, 3H, CH_3SO_2), 2.72 (m, 4H, 1,4-H), 1.81 (m, 4H, 2,3-H). ^{13}C NMR (DMSO- d_6 , 75 MHz): 20.35 (C-4), 21.57 (C-2,3), 22.40 (C-1), 44.49 (CH_3SO_2), 45.11 (4-Cl-C₆H₄-CH₂), 109.85, 110.76, 117.52, 118.88, 126.30, 128.21, 128.65, 131.04, 131.82, 136.91, 138.09, and 138.59 (Ar-C). MS LRMS (ESI): (calc) 387.07 (found) 388.12 (MH)⁺. Anal. Calcd for $\text{C}_{12}\text{H}_{14}\text{N}_2\text{O}_2\text{S}$: C, 64.25; H, 5.39; N, 3.75. Found: C, 64.42; H, 5.26; N, 3.57

Synthesis of 9-[(4-Chlorophenyl)sulfonyl]-6-methylsulfonyl-2,3,4,9-tetrahydro-1H-carbazole (10b)

Tetrahydrocarbazole (249 mg, 1 mmol) was dissolved in dry DMF (3 mL) and the stirred solution was treated with NaH in oil dispersion 60% (21 mg, 0.521 mmol). The reaction mixture was stirred at room temperature for 1 hour and then treated with 4-chlorophenylsulfonyl chloride (274 mg, 0.522 mmol), the stirring was continued at room temperature overnight and then poured onto ice-cold water to give solid product. The solid product filtered off, dried under vacuum and suspended in ether with vigorous shaking then filtered off to give white powder of the corresponding *N*-phenylsulfonyltetrahydrocarbazole.

Yield: 81%, m.p.: 221 °C, IR (KBr) $\nu_{\max}/\text{cm}^{-1}$ 1302 (CH_3SO_2). ^1H NMR (DMSO- d_6 , 300 MHz) δ 8.25 (d, $J=8.8$ Hz, 1H), 8.01 (s, 1H), 7.93 (d, $J=8.4$ Hz, 2H), 7.84 (d, $J=8.8$ Hz, 1H), 7.66 (d, $J=8.5$ Hz, 2H), 3.21 (s, 3H, CH_3SO_2), 2.99 (t, $J=6.3$ Hz, 2H, 1-H), 2.63 (t, $J=5.5$ Hz, 2H, 4-H), 1.85 (m, 2H, 3-H), 1.75 (m, 2H, 2-H). ^{13}C NMR (DMSO- d_6 , 75 MHz): 20.32 (C-4), 21.21 (C-3), 22.51 (C-2), 24.05 (C-1), 43.90 (CH_3SO_2), 114.25, 117.99, 118.75, 122.57, 128.35, 129.74, 130.24, 136.10, 136.13, 137.35, 137.63 and 138.13, 139.86 (Ar-C). MS LRMS (ESI): (calc) 423.04 (found) 424.03 (MH)⁺. Anal. Calcd for $\text{C}_{12}\text{H}_{14}\text{N}_2\text{O}_2\text{S}$: C, 53.83; H, 4.28; N, 3.30. Found: C, 53.66; H, 4.47; N, 3.49

6-(Methylsulfonyl)-1,2,3,9-tetrahydro-4H-carbazol-4-one (11)

Tetrahydrocarbazole (249 mg, 1.0 mmol) was dissolved in 5 mL THF:H₂O (9:1). While the solution of tetrahydrocarbazole was cooled in ice bath, DDQ (454 mg, 2.0 mmol) dissolved in THF (3 mL) was added dropwise with stirring. The temperature of the reaction mixture raised to room temperature, white solid product precipitated out from the solution after 10 min of the stirring and the reaction continued stirring for 2 hours until completion. The precipitate was filtered off and washed with methanol (1 mL) to give fibrous white crystals of the title compound in a pure form with no need for further crystallization.

Yield: 68%, m.p.: 327 °C, IR (KBr) $\nu_{\max}/\text{cm}^{-1}$ 3139 (NH), 1634 (CO), 1291 (CH₃-SO₂). ¹H NMR (DMSO-*d*₆, 300 MHz) δ 12.37 (s, 1H, NH), 8.47 (s, 1H, 5-H), 7.71 (d, *J*=8.6 Hz, 1H, 7-H), 7.63 (d, *J*=8.5 Hz, 1H, 8-H), 3.17 (s, 3H, CH₃SO₂), 3.02 (t, *J*=5.9 Hz, 2H, 1-H), 2.48 (m, 2H, 3-H), 2.15 (m, 2H, 2-H). ¹³C NMR (DMSO-*d*₆, 75 MHz): 22.70 (C-2), 23.19 (C-1), 37.62 (C-3), 44.47 (CH₃SO₂), 112.36, 119.67, 121.13, 123.90, 133.91, 138.25, and 154.94 (Ar-C), 193.13 (CO). MS LRMS (ESI): (calc) 263.06 (found) 264.02 (MH)⁺. Anal. Calcd for C₁₂H₁₄N₂O₂S: C, 59.30; H, 4.98; N, 5.32. Found: C, 59.44; H, 5.10; N, 5.20

Synthesis of 9-(4-chlorobenzoyl)-6-(methylsulfonyl)-1,2,3,9-tetrahydro-4H-carbazol-4-one (12a)

Tetrahydrocarbazole (100 mg, 0.38 mmol) was dissolved in dry DMF (1 mL) and the stirred solution was treated with NaH in oil dispersion 60% (19.7 mg, 0.494 mmol). The reaction mixture was stirred at room temperature for 1 hour and then treated with 4-chlorobenzoyl chloride (0.6 mL, 0.456 mmol), the stirring was continued at room temperature overnight and then poured onto ice-cold water to give solid product. The solid product filtered off, dried under vacuum and suspended in ether with vigorous shaking then filtered off to give white powder of the target *N*-benzoyltetrahydrocarbazole.

Yield: 41%, m.p.: 230 °C, IR (KBr) $\nu_{\max}/\text{cm}^{-1}$ 1707 (CO ketone), 1661 (CO amide), 1303 (CH₃-SO₂). ¹H NMR (DMSO-*d*₆, 300 MHz) δ 8.62 (s, 1H, 5-H), 7.83 (t, *J*=8.9 Hz, 3H, 7-H, 2,6-H), 7.70 (d, *J*=8.1 Hz, 2H, 3,5-H), 7.56 (d, *J*=8.7 Hz, 1H, 8-H), 3.23 (s, 3H, CH₃SO₂), 2.80 (t, *J*=5.8 Hz, 2H, 1-H), 2.55 (t, *J*=6.0 Hz, 2H, 3-H), 2.10 (quintet, *J*=5.8 Hz, 2H, 2-H). ¹³C NMR (DMSO-*d*₆, 75 MHz): 23.27 (C-2), 25.17 (C-1), 37.33 (C-3), 44.08 (CH₃SO₂), 115.18, 115.65, 119.81, 123.02, 125.04, 129.25, 132.03, 136.59, 138.31, 139.13 and 154.76 (Ar-C), 167.71 (CO-N), 194.69 (CO). MS LRMS (ESI): (calc) 437.02 (found) 438.07 (MH)⁺. Anal. Calcd for C₁₂H₁₄N₂O₂S: C, 59.78; H, 4.01; N, 3.49. Found: C, 59.61; H, 3.89; N, 3.68.

Synthesis of 9-(4-chlorobenzyl)-6-(methylsulfonyl)-1,2,3,9-tetrahydro-4H-carbazol-4-one (12b)

Tetrahydrocarbazole (249 mg, 1 mmol) was dissolved in dry DMF (4 mL) and the stirred solution was treated with NaH in oil dispersion 60% (52 g, 0.61 mmol). The reaction mixture was stirred at room temperature for 1 hour and then treated with 4-chlorobenzyl chloride (115 mg, 1.4 mmol), the stirring was continued at room temperature overnight and then poured onto ice-cold water to give oily product. Methanol was added to the resulting oily product dropwise until complete dissolution of the oil in MeOH/H₂O and left standing overnight at room temperature to give off light brown crystals, filtered off and washed with ether (5 mL) affording the corresponding *N*-benzyltetrahydrocarbazole.

Yield: 69%, m.p.: 205-207 °C, IR (KBr) $\nu_{\max}/\text{cm}^{-1}$ 1647 (CO), 1300 (CH₃-SO₂). ¹H NMR (DMSO-*d*₆, 300 MHz) δ 8.55 (s, 1H, 5-H), 7.81 (d, *J*=8.6 Hz, 1H, 7-H), 7.75 (d, *J*=8.6 Hz, 1H, 8-H) 7.40 (dd, *J*=8.0 Hz, 2H, 2,6-H),

7.16 (dd, $J=8.0$ Hz, 2H, 3,5-H), 5.60 (s, 2H, 4-Cl-C₆H₄-CH₂), 3.19 (s, 3H, CH₃SO₂), 3.02 (t, $J=5.5$ Hz, 2H, 3-H), 2.16 (m, 2H, 2-H). ¹³C NMR (DMSO-*d*₆, 75 MHz): 21.75 (C-2), 22.77 (C-1), 37.33 (C-3), 44.32 (CH₃SO₂), 45.99 (Ar-CH₂), 111.52, 112.48, 119.85, 121.41, 123.75, 128.55, 128.83, 132.28, 134.64, 135.46, 138.87 and 155.34 (Ar-C), 193.18 (CO). MS LRMS (ESI): (calc) 387.07 (found) 387.99 (MH)⁺. Anal. Calcd for C₁₂H₁₄N₂O₂S: C, 61.93; H, 4.68; N, 3.61. Found: C, 61.77; H, 4.87; N, 3.79.

Synthesis of 9-[(4-chlorophenyl)sulfonyl]-6-(methylsulfonyl)-1,2,3,9-tetrahydro-4H-carbazol-4-one (12c)

Tetrahydrocarbazole (249 mg, 1 mmol) was dissolved in dry DMF (4 mL) and the stirred solution was treated with NaH in oil dispersion 60% (52 mg, 1.3 mmol). The reaction mixture was stirred at room temperature for 1 hour and then treated with 4-chlorophenylsulfonyl chloride (274 mg, 1.3 mmol), the stirring was continued at room temperature overnight and then poured onto ice-cold water to give oily product. Methanol was added to the resulting oily product dropwise until complete dissolution of the oil in MeOH/H₂O and left standing overnight at room temperature to give off white fibrous crystals, filtered off and washed with ether (5 mL) affording the corresponding *N*-phenylsulfonyltetrahydrocarbazole.

Yield: 58%, m.p.: 253 °C, IR (KBr) $\nu_{\max}/\text{cm}^{-1}$ 1659 (CO), 1301 (CH₃-SO₂). ¹H NMR (DMSO-*d*₆, 300 MHz) δ 8.58 (s, 1H, 5-H), 8.32 (d, $J=8.9$ Hz, 1H, 7-H), 8.14 (dd, $J=8.3$ Hz, 2H, 2,6-H), 7.94 (d, $J=8.8$ Hz, 1H, 8-H), 7.74 (dd, $J=8.3$ Hz, 2H, 3,5-H), 3.41 (t, $J=6.0$ Hz, 2H, 3-H), 3.23 (s, 3H, CH₃SO₂), 2.56 (t, $J=6.0$ Hz, 2H, 1-H), 2.22 (quintet, $J=6.0$ Hz, 2H, 2-H). ¹³C NMR (DMSO-*d*₆, 75 MHz): 22.48 (C-2), 23.89 (C-1), 37.06 (C-3), 43.96 (CH₃SO₂), 114.59, 116.67, 120.18, 124.02, 125.28, 129.03, 130.52, 135.37, 137.08, 137.51, 140.78 and 153.96 (Ar-C), 194.50 (CO). MS LRMS (ESI): (calc) 437.02 (found) 438.05 (MH)⁺. Anal. Calcd for C₁₂H₁₄N₂O₂S: C, 52.11; H, 3.68; N, 3.20. Found: C, 52.29; H, 3.76; N, 3.18.

3.2. Biological activity:

Experimental animals were obtained from Theodor Bilharz Research Institute (TBRI), Egypt and approval of the institutional animal ethical committee for the animals' studies was obtained from the Office of Environmental Health and Radiation Safety, ACUC Protocol 1096-5. The animals were maintained according to accepted standards of animal care.

3.2.1. Human COX-1 and COX-2 enzymatic assay

Human COX-1 and COX-2 activities were determined as described by Wakitani et al[31]. Human COX-1 (0.3 mg protein/assay) or COX-2 (1 mg protein/assay) was suspended in 0.2 ml of 100 mmol trise HCl buffer (pH 8) containing the cofactors, 2 mmol of hematin and 5 mmol of tryptophan. With each compound under investigation individually, the reaction mixture was pre-incubated for 5 min at 24°C. 30 mmol of [¹⁴C]-arachidonic acid (100.00 dpm) was added to the mixture and then incubated for 2 min with COX-1 and 45 min with COX-2 at 24°C. 400 μ l solution of Et₂O/MeOH/1 M citric acid (30:4:1, v/v/v) was added to stop the reaction. The mixture was centrifuged at 1700X/g for 5 min at 4°C, then 50 μ l of the upper phase was applied to a plate of thin layer chromatography (TLC). TLC was exposed at 4°C to a solvent system of Et₂O/MeOH/AcOH (90:2:0.1, v/v/v). Radiometric photographic system was used to determine the percent conversion of arachidonic

acid to PGH2 and its decomposition products, and eventually from which the enzyme activity was calculated. The concentration of the compound causing 50% inhibition (IC_{50}) was calculated.

3.2.2. Carrageenan-induced rat paw edema

Male albino rats weighing 120-150 g were kept in an animal house under standard conditions regarding light, temperature and free access to food and water. Groups of six rats each were subjected to induction of paw edema by subplantar injection of 50 μ l of 2% carrageenan solution in saline (0.9%). Indomethacin and the compounds under investigation were dissolved in DMSO then injected subcutaneously in a dose of 10 μ mol/kg body weight, 1 h earlier than the carrageenan injection. Control group was injected with DMSO only. Plethysmometer were used immediately after carrageenan injection and 4h later to measure the volume of paw edema. The increase in paw volume from 0 to 4 h was measured[32]. The %protection against inflammation was calculated as follows:

$Vc - Vd \times 100 / Vc$ where Vc is the increase in paw volume in the absence of test compound (control) and Vd is the increase in paw volume after injection of the test compound. Data were expressed as the mean \pm SEM. Student's t-test and P values was used to determine the significance in difference between the control and the groups injected with the test compound. The difference in results was considered significant when $P < 0.001$. Taking indomethacin as reference standard compound, the relative anti-inflammatory activity of the test compounds was also calculated.

3.2.3. Estimation of plasma prostaglandin E2 (PGE2)

8 Heparinized blood samples were collected from rats and centrifuged to separate the plasma at 12,000 g for 2 min at 40°C, then immediately frozen, and stored at 20°C until use. The estimation procedure was designed to be competitive immune assay to determine PGE2 quantitatively in the biological fluids using EIA PGE2 kit (Aldrich, Steinheim, Germany). A monoclonal antibody to PGE2 is used by kit to bind competitively to the PGE2 in the sample after a simultaneous incubation at room temperature. The substrate was added after washing the excess reagents away. After a short incubation time, a yellow color generated and got read on a microplate reader DYNATech, MR 5000 at 405 nm (Dynatech Industries Inc., McLean, VA, USA) after stopping the enzyme reaction. The intensity of the bound yellow color is inversely proportional to the concentration of PGE2 in either standard or samples.

3.2.4. Human, Rat, and Dog Microsomal COX Assays

In 50 mM potassium phosphate buffer, pH 7.1, containing 0.1 M NaCl, 2 mM EDTA, and 1 mM phenylmethylsulfonyl fluoride (homogenization buffer), 1–10 g of tissue obtained from the whole kidney were suspended. A hand-held tissue homogenizer (Biospec Products, Inc., Bartlesville, OK) at maximum setting was used to homogenize the samples for 2 min on ice, then the homogenized products were sonicated for 10 s using a micro-ultrasonic cell disrupter (Kontes, Vineland, NJ). Tissue homogenates were then exposed to centrifugation at 100,000g for 1h at 4°C. The 100,000g microsomal pellet was re-suspended in homogenization buffer and was sonicated (2 3 10 s) on ice. Microsomal suspensions of human, rat, and dog kidney got diluted to

protein concentrations of approximately 6, 10, and 12 mg/ml, respectively. Aliquots of microsomal preparations were stored at 280°C and thawed on ice immediately before assays.

The microsomal preparation from rat, dog, or human kidneys was pre-incubated with the reference standard drug, Celecoxib at room temperature for 5 or 15 min. The pre-incubation buffer was composed of protein concentration of 0.12 mg/ml, 0.1 M Trise HCl, pH 7.4, 10 mM EDTA, 0.5mM phenol, 1 mM reduced glutathione, and 1 mM hematin. The final concentration adjusted at 2 mM, then arachidonic acid and the samples were incubated at room temperature for 40 min. The reaction was stopped by the addition of 25 ml of 1 N HCl with mixing after the incubation period. Radioimmunoassay was used to analyze the amount of PGE2 after neutralization of the samples with 25 ml of 1 N NaOH.

Assays were repeated two or three times. Ethanol was used as a vehicle for the control reaction mixtures instead of arachidonic acid. In the control reaction mixture, the levels of PGE2 in samples from human, dog, and rat kidney microsomes were approximately 1.5 ng/mg protein, 0.1 ng/mg protein, and 6.7 ng/mg protein, respectively. In the presence of arachidonic acid, levels of PGE2 in these preparations increased to approximately 4.2 ng/mg protein, 1.2 ng/mg protein, and 22 ng/mg protein, respectively. COX activity in the absence of test compounds is defined as the difference between PGE2 levels in samples incubated in the presence of arachidonic acid or ethanol vehicle.

3.2.5. Cotton pellet-induced granuloma bioassay

120-140 g of adult male Sprague Dawley rats were acclimated one week earlier before use and allowed to unlimited access to standard rat chow and water. Before starting the experiment, the animals were randomly grouped into six animals for each. Cotton pellet (35 ± 1 mg) cut from dental rolls were wet with 0.2 ml (containing 0.01 mmol) of a solution of the compound under the test in chloroform and the solvent was allowed to evaporate. Each cotton pellet was subsequently injected with 0.2 ml of an aqueous solution of antibiotics (1 mg penicillin G and 1.3 mg dihydrostreptomycin/ml). Two pellets, one in each axilla of the rat were implanted under mild general anesthesia, subcutaneously. One group of animals received the standard reference indomethacin and the antibiotics at the same concentration. Control rats were similarly implanted with the pellets containing only the antibiotics. The animals were sacrificed after 7 days and the two cotton pellets, with adhering granulomas, were removed, dried for 48 h at 60 °C and weighed. The difference between the initial and final weight was taken as a measure of granuloma \pm SEM for each group. The percentage reduction in dry weight of granuloma from control value was also calculated. The dose-response curves were set using the doses 4, 7, 10 and 15 μ mol of each compound. Dose-response curve was used to determine the ED₅₀ values.

3.2.6. Ulcerogenic effects

Indomethacin was used as reference standard to test the ulcerogenic potential[33] of all target compounds. 100-120 g of Male albino rats were fasted for 12 h before administration of the compounds. Water was given ad libitum. The animals were randomly grouped into six rats for each. 1% gum acacia were given orally to the control group. Indomethacin or test compounds were given orally to the test groups in two equal doses at 0 and 12 h for three successive days at a dose of 30 μ mol/kg body weight per day. After six hours from the administration of the last dose, animals were sacrificed by diethyl ether and the stomach was removed. An

opening was made at the greater curvature, and the stomach was washed with cold saline to be inspected by a 3_x magnifying lens for any signs of hyperemia, hemorrhage, definite hemorrhagic erosion or ulcer.

The ulcer index was calculated using an arbitrary scale to measure the severity of stomach lesions[33]. The %ulceration for each group was calculated as follows: % Ulceration =Number of animals bearing ulcer in a groupX100/Total number of animals in the same group.

3.3. Molecular docking studies:

All compounds were built and saved as Mol2. The crystal structure of COX-2 enzyme in complex with indomethacin was downloaded from Protein Data Bank (PDB code entry; 4COX). The protein was loaded into Leadit 2.1.2[34] and the receptor components were selected. The binding site was defined by selecting indomethacin as a reference ligand to which all coordinates were computed. Amino acids within radius 6.5 Å^o were selected at the binding site. All chemical ambiguities associated with the residues were left as default. Ligand binding was driven by enthalpy (classic triangle matching). For scoring, all default settings were restored. Intra-ligand clashes were computed by using clash factor of 0.6. The maximum number of solutions per iteration was 200. The maximum value of solution per fragmentation was 200. The base placement method was used as a docking strategy.

3.4. Molecular Dynamics

The best conformation from each docking process of each compound was kept inside the active site. The quality of the temperature-related factors, protein geometries, and electron density was tested. All hydrogens were added and energy minimization was computed. The solvent molecules that were in the system were deleted before solvation; salt atoms were added to ensure complete neutralization of the biomolecular system. The solvent atoms were added to surround the biomolecular system (protein-ligand complex) in a spherical shape. Amber 10:EHT was selected as a force field in the potential setup step. All Van der Waals forces, electrostatics, and restraints were enabled. The heat was adjusted in order to increase the temperature of the system from 0-300 K which was followed by equilibration and production for 300 ps; cooling was then initiated until to 0 K was reached.

3.5. MM/GBVI and TPSA calculation

These were calculated after molecular docking with MOE[35]. Placement method was used as Alpha Triangle, timeout (seconds) = 300, minimum iterations = 8000 and max iterations = 500000. Rescoring was done by affinity dG, hydrogen bonds = -0.65, hydrophobic contacts = -0.01235, ionic contact =1, Metal ligation =1, and hydrophobic –polar = 0.02497. The refinement was selected as Grid Mn, in which elec. Cutoff =5.5, VDW cutoff = 4, and VDW potential was enabled. After that the best pose was kept inside the active site. No ligands other than the best conformation were kept. TPSA, Affinity pki, were then computed.

[1] P.J. Loll, Structure of prostaglandin H₂ synthase-1 (COX-1) and its NSAID binding sites, in: N. Bazan, J. Botting, J. Vane (Eds.) *New Targets in Inflammation: Inhibitors of COX-2 or Adhesion Molecules* Proceedings of a conference held on April 15–16, 1996, in New Orleans, USA, supported by an educational grant from Boehringer Ingelheim, Springer Netherlands, Dordrecht, 1996, pp. 13-21.

- [2] G. Rimon, R.S. Sidhu, D.A. Lauver, J.Y. Lee, N.P. Sharma, C. Yuan, R.A. Frieler, R.C. Trievel, B.R. Lucchesi, W.L. Smith, Coxibs interfere with the action of aspirin by binding tightly to one monomer of cyclooxygenase-1, *Proceedings of the National Academy of Sciences of the United States of America*, 107 (2010) 28-33.
- [3] J.R. Vane, J.A. Mitchell, I. Appleton, A. Tomlinson, D. Bishop-Bailey, J. Croxtall, D.A. Willoughby, Inducible isoforms of cyclooxygenase and nitric-oxide synthase in inflammation, *Proceedings of the National Academy of Sciences of the United States of America*, 91 (1994) 2046-2050.
- [4] N. Zidar, K. Odar, D. Glavac, M. Jerse, T. Zupanc, D. Stajer, Cyclooxygenase in normal human tissues is COX-1 really a constitutive isoform, and COX-2 an inducible isoform?, *Journal of Cellular and Molecular Medicine*, 13 (2009) 3753-3763.
- [5] N.S. Kirkby, A.K. Zaiss, W.R. Wright, J. Jiao, M.V. Chan, T.D. Warner, H. R. Herschman, J.A. Mitchell, Differential COX-2 induction by viral and bacterial PAMPs: Consequences for cytokine and interferon responses and implications for anti-viral COX-2 directed therapies, *Biochemical and Biophysical Research Communications*, 438 (2013) 249-256.
- [6] W.L. Smith, Y. Urade, P.-J. Jakobsson, Enzymes of the cyclooxygenase pathways of prostanoïd biosynthesis, *Chemical Reviews*, 111 (2011) 5821-5865.
- [7] A. Zarghi, S. Arfaei, Selective COX-2 inhibitors: A review of their structure-activity relationships, *Iranian Journal of Pharmaceutical Research*, 10 (2011) 655-683.
- [8] J.P. Peesa, P.R. Yalavarthi, A. Rasheed, V.B.R. Mandava, A perspective review on role of novel NSAID prodrugs in the management of acute inflammation, *Journal of Acute Disease*, 5 (2016) 364-381.
- [9] C.A. Rouzer, L.J. Marnett, Cyclooxygenases: structural and functional insights, *Journal of Lipid Research*, 50 (2009) S29-S34.
- [10] R.G. Kurumbail, A.M. Stevens, J.K. Gierse, J.J. McDonald, R.A. Stegeman, J.Y. Pak, D. Gildehaus, J.M. Miyashiro, T.D. Penning, K. Seibert, P.C. Isakson, W.C. Stallings, Structural basis for selective inhibition of cyclooxygenase-2 by anti-inflammatory agents, *Nature*, 384 (1996) 644-648.
- [11] D. Picot, P.J. Loll, R.M. Garavito, The X-ray crystal structure of the membrane protein prostaglandin H2 synthase-1, *Nature*, 367 (1994) 243-249.
- [12] A.L. Blobaum, L.J. Marnett, Structural and functional basis of cyclooxygenase inhibition, *Journal of Medicinal Chemistry*, 50 (2007) 1425-1441.
- [13] R. Anana, P.N.P. Rao, Q.-H. Chen, E.E. Knaus, Synthesis and biological evaluation of linear phenylethynylbenzenesulfonamide regioisomers as cyclooxygenase-1/-2 (COX-1/-2) inhibitors, *Bioorganic & Medicinal Chemistry*, 14 (2006) 5259-5265.
- [14] J.K. Gierse, J.J. McDonald, S.D. Hauser, S.H. Rangwala, C.M. Koboldt, K. Seibert, A single amino acid difference between cyclooxygenase-1 (COX-1) and -2 (COX-2) reverses the selectivity of COX-2 specific inhibitors, *The Journal of Biological Chemistry*, 271 (1996) 15810-15814.
- [15] K.M. Knights, A.A. Mangoni, J.O. Miners, Defining the COX inhibitor selectivity of NSAIDs: Implications for understanding toxicity, *Expert Review of Clinical Pharmacology*, 3 (2010) 769-776.
- [16] A.K. Dwivedi, V. Gurjar, S. Kumar, N. Singh, Molecular basis for nonspecificity of nonsteroidal anti-inflammatory drugs (NSAIDs), *Drug Discovery Today*, 20 (2015) 863-873.
- [17] S. Moncada, E.A. Higgs, J.R. Vane, Human arterial and venous tissues generate prostacyclin (prostaglandin X), a protein inhibitor of platelet aggregation, *The Lancet*, 309 (1977) 18-21.
- [18] J.N. Topper, J. Cai, D. Falb, M.A. Gimbrone, Jr., Identification of vascular endothelial genes differentially responsive to fluid mechanical stimuli: Cyclooxygenase-2, manganese superoxide dismutase, and endothelial cell nitric oxide synthase are selectively up-regulated by steady laminar shear stress, *Proceedings of the National Academy of Sciences of the United States of America*, 93 (1996) 10417-10422.
- [19] M.S. Estevão, L.C.R. Carvalho, M. Freitas, A. Gomes, A. Viegas, J. Manso, S. Erhardt, E. Fernandes, E.J. Cabrita, M.M.B. Marques, Indole based cyclooxygenase inhibitors: Synthesis, biological evaluation, docking and NMR screening, *European Journal of Medicinal Chemistry*, 54 (2012) 823-833.
- [20] W.C. Black, C. Bayly, M. Belley, C.C. Chan, S. Charleson, D. Denis, J.Y. Gauthier, R. Gordon, D. Guay, S. Kargman, C.K. Lau, Y. Leblanc, J. Mancini, M. Ouellet, D. Percival, P. Roy, K. Skorey,

- P. Tagari, P. Vickers, E. Wong, L. Xu, P. Prasit, From indomethacin to a selective COX-2 inhibitor: Development of indolalkanoic acids as potent and selective cyclooxygenase-2 inhibitors, *Bioorganic & Medicinal Chemistry Letters*, 6 (1996) 725-730.
- [21] C. Luo, M.L. He, L. Bohlin, Is COX-2 a perpetrator or a protector? Selective COX-2 inhibitors remain controversial, *Acta Pharmacologica Sinica*, 26 (2005) 926-933.
- [22] G. Carullo, F. Galligano, F. Aiello, Structure-activity relationships for the synthesis of selective cyclooxygenase 2 inhibitors: An overview (2009-2016), *MedChemComm*, 8 (2017) 492-500.
- [23] M.C. Walker, R.G. Kurumbail, J.R. Kiefer, K.T. Moreland, C.M. Koboldt, P.C. Isakson, K. Seibert, J.K. Gierse, A three-step kinetic mechanism for selective inhibition of cyclo-oxygenase-2 by diarylheterocyclic inhibitors, *Biochemical Journal*, 357 (2001) 709-718.
- [24] D.K. Bhattacharyya, M. Lecomte, C.J. Rieke, M. Garavito, W.L. Smith, Involvement of arginine 120, glutamate 524, and tyrosine 355 in the binding of arachidonate and 2-phenylpropionic acid inhibitors to the cyclooxygenase active site of ovine prostaglandin endoperoxide H synthase-1, *The Journal of Biological Chemistry*, 271 (1996) 2179-2184.
- [25] J. Grover, N. Bhatt, V. Kumar, N.K. Patel, B.J. Gondaliya, M. Elizabeth Sobhia, K.K. Bhutani, S.M. Jachak, 2,5-Diaryl-1,3,4-oxadiazoles as selective COX-2 inhibitors and anti-inflammatory agents, *RSC Advances*, 5 (2015) 45535-45544.
- [26] D.A. Al-Turki, M.A. Al-Omar, L.A. Abou-zeid, I.A. Shehata, M.S. Al-Awady, Design, synthesis, molecular modeling and biological evaluation of novel diaryl heterocyclic analogs as potential selective cyclooxygenase-2 (COX-2) inhibitors, *Saudi Pharmaceutical Journal*, 25 (2017) 59-69.
- [27] S.J. Wey, M.E. Augustyniak, E.D. Cochran, J.L. Ellis, X. Fang, D.S. Garvey, D.R. Janero, L.G. Letts, A.M. Martino, T.L. Melim, M.G. Murty, S.K. Richardson, J.D. Schroeder, W.M. Selig, A.M. Trocha, R.S. Wexler, D.V. Young, I.S. Zemtseva, B.M. Zifcak, Structure-based design, synthesis, and biological evaluation of indomethacin derivatives as cyclooxygenase-2 inhibiting nitric oxide donors, *Journal of Medicinal Chemistry*, 50 (2007) 6367-6382.
- [28] B. Weng, R. Liu, J.-H. Li, An improved method for the synthesis of carbazolones by palladium/copper-catalyzed intramolecular annulation of *N*-arylenaminones, *Synthesis*, 2010 (2010) 2926-2930.
- [29] G.K. Mittapalli, F. Zhao, A. Jackson, H. Gao, H. Lee, S. Chow, M.P. Kaur, N. Nguyen, R. Zamboni, J. McKelvy, F. Wong-Staal, J.E. Macdonald, Discovery of ITX 4520: A highly potent orally bioavailable hepatitis C virus entry inhibitor, *Bioorganic & Medicinal Chemistry Letters*, 22 (2012) 4955-4961.
- [30] Y. Oikawa, O. Yonemitsu, Selective oxidation of the side chain at C-3 of indoles, *The Journal of Organic Chemistry*, 42 (1977) 1213-1216.
- [31] K. Wakitani, T. Nanayama, M. Masaki, M. Matsushita, Profile of JTE-522 as a human cyclooxygenase-2 inhibitor, *Japanese Journal of Pharmacology*, 78 (1998) 365-371.
- [32] M. Di Rosa, D.A. Willoughby, Screens for anti-inflammatory drugs, *The Journal of Pharmacy and Pharmacology*, 23 (1971) 297-298.
- [33] M.S. Abouzeit-Har, T. Verimer, J.P. Long, Effect of long term estrogen and lithium treatment on restraint induced gastric erosion in intact and ovariectomized rats, *Pharmazie*, 37 (1982) 593-595.
- [34] M. Rarey, B. Kramer, T. Lengauer, G. Klebe, A fast flexible docking method using an incremental construction algorithm, *Journal of Molecular Biology*, 261 (1996) 470-489.
- [35] S. Vilar, G. Cozza, S. Moro, Medicinal chemistry and the molecular operating environment (MOE): Application of QSAR and molecular docking to drug discovery, *Current Topics in Medicinal Chemistry*, 8 (2008) 1555-1572.

Research highlights:

- New ring-extended indomethacin analogs were designed on structural basis.
- Ring extension, deletion of COOH and introduction of CH₃SO₂ gave selective COX-2 inhibitors.
- New inhibitors showed observed diminishing to PGE₂ plasma levels.
- The docking scores of the new inhibitors were highly correlated to its IC₅₀ values.
- The new perspective of molecular design facilitates elaboration of more selective inhibitors.